



**HAL**  
open science

## A closed-form extension to the Black-Cox model

Aurélien Alfonsi, Jérôme Lelong

► **To cite this version:**

Aurélien Alfonsi, Jérôme Lelong. A closed-form extension to the Black-Cox model. *International Journal of Theoretical and Applied Finance*, 2012, 15 (8), pp.1250053:1-30. 10.1142/S0219024912500537. hal-00414280v2

**HAL Id: hal-00414280**

**<https://hal.science/hal-00414280v2>**

Submitted on 29 Mar 2010

**HAL** is a multi-disciplinary open access archive for the deposit and dissemination of scientific research documents, whether they are published or not. The documents may come from teaching and research institutions in France or abroad, or from public or private research centers.

L'archive ouverte pluridisciplinaire **HAL**, est destinée au dépôt et à la diffusion de documents scientifiques de niveau recherche, publiés ou non, émanant des établissements d'enseignement et de recherche français ou étrangers, des laboratoires publics ou privés.

# A closed-form extension to the Black-Cox model

Aurélien Alfonsi and Jérôme Lelong

Université Paris-Est, CERMICS, Project team MathFi ENPC-INRIA-UMLV, Ecole des Ponts,  
6-8 avenue Blaise Pascal, 77455 Marne La Vallée, France.  
`alfonsi@cermics.enpc.fr`

Ecole Nationale Supérieure de Techniques Avancées ParisTech, Unité de Mathématiques Ap-  
pliquées, 42 bd Victor 75015 Paris, France.  
Laboratoire Jean Kuntzmann, Université de Grenoble et CNRS, BP 53, 38041 Grenoble Cédex 9,  
FRANCE.  
e-mail : `jerome.lelong@imag.fr`

March 29, 2010

## Abstract

In the Black-Cox model, a firm defaults when its value hits an exponential barrier. Here, we propose an hybrid model that generalizes this framework. The default intensity can take two different values and switches when the firm value crosses a barrier. Of course, the intensity level is higher below the barrier. We get an analytic formula for the Laplace transform of the default time. This result can be also extended to multiple barriers and intensity levels. Then, we explain how this model can be calibrated to Credit Default Swap prices and show its tractability on different kinds of data. We also present numerical methods to numerically recover the default time distribution.

*Keywords:* *Credit Risk, Intensity Model, Structural Model, Black-Cox Model, Hybrid Model, Parisian options, ParAsian options.*

**Acknowledgments.** We would like to thank Jérôme Brun and Julien Guyon from Société Générale for providing us with market data and discussions. We also thank the participants of the conference “Recent Advancements in the Theory and Practice of Credit Derivatives”(Nice, September 2009) and especially Monique Jeanblanc, Alexander Lipton and Claude Martini for fruitful remarks. Aurélien Alfonsi would like to acknowledge the support of the “Chaire Risques Financiers” of Fondation du Risque.

# 1 Introduction and model setup

Modelling firm defaults is one of the fundamental matter of interest in finance. It has stimulated research over the past decades. Clearly, the recent worldwide financial crisis and its bunch of resounding bankruptcies have underlined once again the need to better understand credit risk. In this paper, we focus on the modelling of a single default. Usually, these models are divided into two main categories: structural and reduced form (or intensity) models.

Structural models aim at explaining the default time with economic variables. In his path breaking work, Merton [16] connected the default of a firm with its ability to pay back its debt. The firm value is defined as the sum of the equity value and the debt value, and is supposed to be a geometric Brownian motion. At the bond maturity, default occurs if the debtholders cannot be reimbursed. In this framework, the equity value is seen as a call option on the firm value. Then, Black and Cox [5] have extended this framework by triggering the default as soon as the firm value goes below some critical barrier. Thus, the default can occur at any time and not only at the bond maturity. Many extensions of the Black Cox model, based on first passage time, have been proposed in the literature. We refer to the book of Bielecki and Rutkowski [4] for a nice overview. Recently, attention has been paid to the calibration of these models to Credit Default Swap (CDS in short) data (Brigo and Morini [7], Dorfleitner et al. [13]). However, though economically sounded, these models can hardly be used intensively on markets to manage portfolios especially for hedging. Unless considering dynamics with jumps (see Zhou [20] for example), their major drawback is that the default time is predictable and no default can occur when the firm value is clearly above the barrier. In other words, they underestimate default probabilities and credit spreads for short maturities.

The principle of reduced form models is to describe the dynamics of the instantaneous probability of default that is also called intensity. This intensity is described by some autonomous dynamics and the default event is thus not related to any criterion on the solvency of the firm. We refer to the book of Bielecki and Rutkowski [4] for an overview of these models. In general, they are designed for being easily calibrated to CDS market data and are in practice more tractable to manage portfolios.

However, none of these two kinds of model is fully satisfactory. In first passage time models, the default intensity is zero away from the barrier and the default event can be forecast. Intensity models are in line with CDS market data, but remain disconnected to the rationales of the firm like its debt and equity values. Thus, they cannot exploit the information available on equity markets. To overcome this shortcoming, and to provide a unified framework for pricing equity and credit products, hybrid models have been introduced, assuming that the default intensity is a (decreasing) function of the stock. Here, we mention the works of Atlan and Leblanc [2], and Carr and Linetsky [8] who consider the case of a defaultable constant elasticity model.

In this paper, we propose an hybrid model, which extends the Black-Cox model and in which the default intensity depends on the firm value. We present in this introduction a simple version of it, and the full model is given in Section 2. We consider the usual

framework when dealing with credit risk and firm value models. Namely, we assume that we are under a risk-neutral probability measure  $\mathbb{P}$  and that the (riskless) short interest rate is constant and equal to  $r > 0$ . We denote by  $(\mathcal{F}_t, t \geq 0)$  the default-free filtration and consider a  $(\mathcal{F}_t)$ -Brownian motion  $(W_t, t \geq 0)$ . We assume that the firm value  $(V_t, t \geq 0)$  evolves according to the Black-Scholes model and therefore satisfies the following dynamics:

$$dV_t = rV_t dt + \sigma V_t dW_t, \quad t \geq 0, \quad (1)$$

where  $\sigma > 0$  is the volatility coefficient. To model the default event, we assume that the default intensity has the following form:

$$\lambda_t = \mu_2 \mathbf{1}_{\{V_t < C e^{\alpha t}\}} + \mu_1 \mathbf{1}_{\{V_t \geq C e^{\alpha t}\}}, \quad (2)$$

where  $C > 0$ ,  $\alpha \in \mathbb{R}$ , and  $\mu_2 > \mu_1 \geq 0$ . This means that the firm has an instantaneous probability of default equal to  $\mu_2$  or  $\mu_1$  depending on whether its value is below or above the time-varying barrier  $C e^{\alpha t}$ . More precisely, let  $\xi$  denote an exponential random variable of parameter 1 independent of the filtration  $\mathcal{F}$ . Then, we define the default time of the firm by:

$$\tau = \inf\{t \geq 0, \int_0^t \lambda_s ds \geq \xi\}. \quad (3)$$

As usual, we also introduce  $(\mathcal{H}_t, t \geq 0)$  the filtration generated by the process  $(\tau \wedge t, t \geq 0)$  and define  $\mathcal{G}_t = \mathcal{F}_t \vee \mathcal{H}_t$ , so that  $(\mathcal{G}_t, t \geq 0)$  embeds both default-free and defaultable information.

This framework is a natural extension of the pioneering Black-Cox model introduced in [5], which can indeed be simply seen as the limiting case of our model when  $\mu_1 = 0$  and  $\mu_2 \rightarrow +\infty$ . In the work of Black and Cox, bankruptcy can in addition happen at the maturity date of the bonds issued by the firm when the firm value is below some level. Here, we do not consider this possibility, even though it is technically feasible, because it would make the default predictable in some cases. In the Black-Cox model, the barrier  $C e^{\alpha t}$  is meant to be a safety covenant under which debtholders can ask for being reimbursed. Here, default can happen either above or below the barrier, which represents instead the border between two credit grades. Let us briefly explain what typical parameter configurations could be for this model. For a very safe firm, we expect that its value start above the barrier with  $\mu_1$  very close to 0. The parameter  $\mu_2$  should also be rather small since it cannot be downgraded too drastically. Instead, for firms that are close to bankruptcy, we expect to have  $C < V_0$  and a high intensity of default  $\mu_2$ . Then, the parameters should be such that the firm is progressively drifted to the less risky region (i.e.  $r - \sigma^2/2 - \alpha > 0$ ). In fact, the CDS prices often reflect two possible outcomes in such critical situations. Either the firm makes bankruptcy in the next future, or it survives and is then strengthened (see Brigo and Morini [7] for the Parmalat crisis case).

Now, we state the main theoretical result on which this paper is based. It gives the explicit formula for the Laplace transform of the default time distribution.

**Theorem 1.1.** *Let us set  $b = \frac{1}{\sigma} \log(C/V_0)$ ,  $m = \frac{1}{\sigma}(r - \alpha - \sigma^2/2)$  and  $\mu_b = \mu_2 \mathbf{1}_{\{b>0\}} + \mu_1 \mathbf{1}_{\{b \leq 0\}}$ . The default cumulative distribution function  $\mathbb{P}(\tau \leq t)$  is a function of  $t$ ,  $b$ ,  $m$ ,  $\mu_1$  and  $\mu_2$  and is fully characterized by its Laplace transform defined for  $z \in \mathbb{C}_+ := \{z \in \mathbb{C}, \Re(z) > 0\}$ ,*

$$\int_0^\infty e^{-zt} \mathbb{P}(\tau \leq t) dt = e^{mb - |b| \sqrt{2(z + \mu_b) + m^2}} \left( \frac{1}{z + \mu_1} - \frac{1}{z + \mu_2} \right) \times \left\{ -\mathbf{1}_{\{b>0\}} + \frac{-m + \sqrt{2(z + \mu_2) + m^2}}{\sqrt{2(z + \mu_1) + m^2} + \sqrt{2(z + \mu_2) + m^2}} \right\} + \frac{1}{z} - \frac{1}{z + \mu_b}. \quad (4)$$

Theorem 1.1 can actually fit in the framework of Theorem 2.1 with  $n = 2$ , where the intensity can take  $n \geq 2$  different values instead of 2. Hence, we refer the reader to Section 2 for a proof of Theorem 1.1, which in fact comes from a result by Kac. Then, our point of view in this paper is to take advantage of this result and obtain a fast calibration procedure to CDS market data.

The Laplace transform (4) can also be obtained thanks to the results on Parisian options by Chesney et al. [11]. This was done in a former version of this paper available on <http://hal.archives-ouvertes.fr>. The default time  $\tau$ , defined by (3), is related to the time spent below and above the barrier. Other Black-Cox extensions based on analytical formulas for Parisian type options have been proposed in the recent past. Namely, Chen and Suchaneki [10], Moraux [17] and Yu [19] considered the case where the default is triggered when the stock has spent a certain amount of time in a row or not under the barrier. Nonetheless, both extensions present the drawback that the default is actually predictable and the default intensity is either 0 or non-finite. This does not hold in our framework.

The paper is structured as follows. In Section 2, we present the full model for which the intensity can take  $n \geq 2$  different values and we obtain a closed formula for the Laplace transform of the default time. Section 3 is devoted to the pricing of CDS and states simple but interesting properties of the CDS spreads in function of the model parameters. Then, we focus on the calibration issue. Section 4 is devoted to the calibration of the model presented above while in Section 5, we discuss the calibration of the full model with  $n \geq 3$ . We present a general calibration procedure for the model and show on different practical settings how the model can fit the market data. We find our calibration results rather encouraging. Last, we give in Section 6 two methods to numerically invert the Laplace transform of the default cumulative distribution function given by Theorems 1.1 and 2.1. For each method, we state in a precise way its accuracy which heavily relies on the regularity of the function to be recovered. The required regularity assumptions are actually proved to be satisfied by the default cumulative distribution function in Appendix A.

## 2 The Laplace transform of the default distribution

In the introduction, we have considered a default intensity which takes two different values depending on whether the firm value is below or above some barrier. Here, we present the full model where the default intensity can take  $n \geq 2$  different values,

$$0 \leq \mu_1 < \dots < \mu_n. \quad (5)$$

We set  $C_0 = +\infty$  and  $C_n = 0$ , and consider  $C_1, \dots, C_{n-1}$  such that  $C_n < C_{n-1} < \dots < C_1 < C_0$ . At time  $t \geq 0$ , we assume that the default intensity of the firm is equal to  $\mu_i$ , when its value is between  $C_i e^{\alpha t}$  and  $C_{i-1} e^{\alpha t}$ . Thus, we set

$$\lambda_t = \sum_{i=1}^n \mu_i \mathbf{1}_{\{C_i e^{\alpha t} \leq V_t < C_{i-1} e^{\alpha t}\}}, \quad (6)$$

and we define the default time  $\tau$  exactly as in (3). Assumption (5) means that the default intensity is increased (resp. decreased) each time it crosses downward (resp. upward) a barrier. Heuristically, these constant intensities can be related to the credit grades of the firm. For a firm in difficulty, crossing downward the barriers can also represent the different credit events that precede a bankruptcy.

Now, we introduce notations that will be used throughout the paper. We set  $m = r - \alpha - \sigma^2/2$  and

$$b_0 = +\infty, \quad b_i = \frac{1}{\sigma} \log(C_i/V_0), \quad i = 1, \dots, n-1 \quad \text{and} \quad b_n = -\infty. \quad (7)$$

Thus, the default intensity (6) is equal to

$$\lambda_t = \sum_{i=1}^n \mu_i \mathbf{1}_{\{b_i \leq W_t + mt < b_{i-1}\}}. \quad (8)$$

From (3), we have

$$\mathbb{P}(\tau > t) = \mathbb{E} \left[ e^{-\int_0^t \sum_{i=1}^n \mu_i \mathbf{1}_{\{b_i \leq W_s + ms < b_{i-1}\}} ds} \right]. \quad (9)$$

Therefore, the default distribution (and its Laplace transform) only depend on  $\mathbf{b} = (b_i)_{i=1, \dots, n-1}$ ,  $m$  and  $\boldsymbol{\mu} = (\mu_i)_{i=1, \dots, n}$ . We set for  $t \geq 0$  and  $z \in \mathbb{C}_+$

$$P_{\mathbf{b}, m, \boldsymbol{\mu}}(t) = \mathbb{P}(\tau \leq t) \quad \text{and} \quad P_{\mathbf{b}, m, \boldsymbol{\mu}}^c(t) = \mathbb{P}(\tau > t) = 1 - P_{\mathbf{b}, m, \boldsymbol{\mu}}(t), \quad (10)$$

$$L_{\mathbf{b}, m, \boldsymbol{\mu}}(z) = \int_0^{+\infty} e^{-zt} \mathbb{P}(\tau \leq t) dt \quad \text{and} \quad L_{\mathbf{b}, m, \boldsymbol{\mu}}^c(z) = 1/z - L_{\mathbf{b}, m, \boldsymbol{\mu}}(z), \quad (11)$$

that are respectively the cumulative distribution function, the survival probability function and their Laplace transforms. When  $n = 2$ , we use the same notations as in the introduction and simply denote by  $b = \log(C_1/V_0)/\sigma$  the barrier level. We also respectively denote by  $P_{b, m, \mu_1, \mu_2}(t)$ ,  $P_{b, m, \mu_1, \mu_2}^c(t)$ ,  $L_{b, m, \mu_1, \mu_2}(z)$  and  $L_{b, m, \mu_1, \mu_2}^c(z)$  the quantities defined in (10) and (11).

The following theorem gives a straightforward way to compute the Laplace transform  $L_{\mathbf{b}, m, \boldsymbol{\mu}}(z)$ .

**Theorem 2.1.** *In the above setting,  $L_{\mathbf{b},m,\boldsymbol{\mu}}(z)$  is given for  $z \in \mathbb{C}_+$  by*

$$L_{\mathbf{b},m,\boldsymbol{\mu}}(z) = \sum_{i=1}^n \mathbf{1}_{\{b_i \leq 0 < b_{i-1}\}} \left\{ \frac{1}{z} - \frac{1}{z + \mu_i} - \beta_i^+ - \beta_i^- \right\},$$

where  $R_{\pm}(\mu) = -m \pm \sqrt{m^2 + 2(z + \mu)}$ . The coefficients  $\beta_i = [\beta_i^- \ \beta_i^+]'$  are uniquely determined by the induction:

$$\beta_i = \Pi_{i-1} \beta_1 + v_{i-1}, \quad i = 1, \dots, n \quad (12)$$

and the conditions  $\beta_1^+ = \beta_n^- = 0$ . Here,  $\Pi_0 = Id$  and  $\Pi_i = P_i \times \dots \times P_1$ ,  $v_0 = 0$  and  $v_i = A^{-1}(\mu_{i+1}, b_i) \left[ \frac{1}{z + \mu_i} - \frac{1}{z + \mu_{i+1}} \ 0 \right]' + P_i v_{i-1}$  with:

$$P_i = \frac{1}{[R_+(\mu_{i+1}) - R_-(\mu_{i+1})]} \times \quad (13)$$

$$\begin{bmatrix} (R_+(\mu_{i+1}) - R_-(\mu_i)) e^{b_i(R_-(\mu_i) - R_-(\mu_{i+1}))} & (R_+(\mu_{i+1}) - R_+(\mu_i)) e^{b_i(R_+(\mu_i) - R_-(\mu_{i+1}))} \\ (R_-(\mu_i) - R_-(\mu_{i+1})) e^{b_i(R_-(\mu_i) - R_+(\mu_{i+1}))} & (R_+(\mu_i) - R_-(\mu_{i+1})) e^{b_i(R_+(\mu_i) - R_+(\mu_{i+1}))} \end{bmatrix}$$

and

$$A^{-1}(\mu_{i+1}, b_i) = \frac{1}{R_+(\mu_{i+1}) - R_-(\mu_{i+1})} \begin{bmatrix} R_+(\mu_{i+1}) e^{-R_-(\mu_{i+1})b_i} & -e^{-R_-(\mu_{i+1})b_i} \\ -R_-(\mu_{i+1}) e^{-R_+(\mu_{i+1})b_i} & e^{-R_+(\mu_{i+1})b_i} \end{bmatrix}.$$

To solve the induction, one has first to determine  $\beta_1^-$  by using that  $\beta_1^+ = \beta_n^- = 0$  and (12) with  $i = n$ . Then, all the  $\beta_i$  can be obtained with (12). When there is only one barrier (i.e.  $n = 2$ ), this can be solved explicitly and the solution is given in Theorem 1.1.

*Proof.* We introduce for  $x \in \mathbb{R}$  and  $t \geq 0$ ,  $X_t^x = x + W_t + mt$ ,

$$\boldsymbol{\lambda}(x) = \sum_{i=1}^n \mu_i \mathbf{1}_{\{x_i \leq x < x_{i-1}\}} \text{ and } p(t, x) = \mathbb{E} \left[ e^{-\int_0^t \boldsymbol{\lambda}(X_s^x) ds} \right].$$

From (3) and (8),  $p(t, 0) = \mathbb{P}(\tau > t)$  is the survival probability function of  $\tau$ .

Thanks to the Girsanov theorem, we have  $p(t, x) = e^{-mx} \tilde{\mathbb{E}} \left[ e^{mX_t^x - m^2 t/2} e^{-\int_0^t \boldsymbol{\lambda}(X_s^x) ds} \right]$  where  $X_t^x$  is a Brownian motion starting from  $x$  under  $\tilde{\mathbb{P}}$ . For  $z > 0$ , we consider the Laplace transform of  $p(t, x)$ :

$$x \in \mathbb{R}, z > 0, L^c(z, x) = \int_0^\infty e^{-zt} p(t, x) dt = e^{-mx} \tilde{\mathbb{E}} \left[ \int_0^\infty e^{-(z+m^2/2)t} e^{mX_t^x - \int_0^t \boldsymbol{\lambda}(X_s^x) ds} dt \right].$$

Now, from a result by Kac ([14], Theorem 4.9 p.271), it comes out that the Laplace transform  $L^c(z, x)$  is  $\mathcal{C}^1$  and piecewise  $\mathcal{C}^2$  w.r.t.  $x$ , and solves:

$$\forall i \in \{1, \dots, n\}, b_i \leq x < b_{i-1}, 1 - (z + \mu_i) L^c(z, x) + m \partial_x L^c(z, x) + \frac{1}{2} \partial_x^2 L^c(z, x) = 0. \quad (14)$$

This is a piecewise affine ODE of order 2 which admits the following solutions:

$$b_i \leq x < b_{i-1}, \quad L^c(z, x) = \frac{1}{z + \mu_i} + \beta_i^- e^{R_-(\mu_i)x} + \beta_i^+ e^{R_+(\mu_i)x}.$$

Now, we write that the Laplace transform is  $\mathcal{C}^1$  at  $b_i$  for  $i = 1, \dots, n-1$ :

$$\begin{cases} \beta_i^- e^{R_-(\mu_i)b_i} + \beta_i^+ e^{R_+(\mu_i)b_i} = \frac{1}{z + \mu_{i+1}} - \frac{1}{z + \mu_i} + \beta_{i+1}^- e^{R_-(\mu_{i+1})b_i} + \beta_{i+1}^+ e^{R_+(\mu_{i+1})b_i} \\ \beta_i^- R_-(\mu_i) e^{R_-(\mu_i)b_i} + \beta_i^+ R_+(\mu_i) e^{R_+(\mu_i)b_i} = \beta_{i+1}^- R_-(\mu_{i+1}) e^{R_-(\mu_{i+1})b_i} + \beta_{i+1}^+ R_+(\mu_{i+1}) e^{R_+(\mu_{i+1})b_i} \end{cases}. \quad (15)$$

We rewrite this in a matrix form:

$$A(\mu_i, b_i) \begin{bmatrix} \beta_i^- \\ \beta_i^+ \end{bmatrix} = \begin{bmatrix} \frac{1}{z + \mu_{i+1}} - \frac{1}{z + \mu_i} \\ 0 \end{bmatrix} + A(\mu_{i+1}, b_i) \begin{bmatrix} \beta_{i+1}^- \\ \beta_{i+1}^+ \end{bmatrix}, \quad A(\mu, x) = \begin{bmatrix} e^{R_-(\mu)x} & e^{R_+(\mu)x} \\ R_-(\mu) e^{R_-(\mu)x} & R_+(\mu) e^{R_+(\mu)x} \end{bmatrix}. \quad (16)$$

We set for  $i = 1, \dots, n-1$ ,  $P_i = A^{-1}(\mu_{i+1}, b_i)A(\mu_i, b_i)$ , which is given in explicit form in (13). We also set

$$v_0 = 0, v_i = A^{-1}(\mu_{i+1}, b_i) \begin{bmatrix} \frac{1}{z + \mu_i} - \frac{1}{z + \mu_{i+1}} & 0 \end{bmatrix}' + P_i v_{i-1} \text{ and } \Pi_0 = Id, \Pi_i = P_i \dots P_1,$$

for  $i = 1 \dots n-1$ . We have that  $\beta_n = \Pi_{n-1}\beta_1 + v_{n-1}$ . Since  $L^c(z, +\infty) = 1/(z + \mu_1)$  and  $L^c(z, -\infty) = 1/(z + \mu_n)$ , we have  $\beta_1^+ = 0$  and  $\beta_n^- = 0$ . In particular,  $(\Pi_{n-1})_{1,1}\beta_1^- + (v_{n-1})_1 = 0$  which uniquely determines  $\beta_1^-$  and gives that  $(\Pi_{n-1})_{1,1} \neq 0$  since  $L^c(z, x)$  is the unique solution of (14) (we can show indeed that  $(\Pi_{n-1})_{1,1} > 0$  because the entries of  $P_i$  are positive). Then, the coefficients  $\beta_i$  are also uniquely determined for  $i = 1, \dots, n$ .

Now, we observe that the formula obtained for  $L^c(z, x)$  when  $z > 0$  remains valid for  $z \in \mathbb{C}_+$  since it is the only possible analytical extension. Last, we conclude using that  $L^c(z, 0) = L_{b, m, \mu}^c(z)$  for  $z \in \mathbb{C}_+$ , since  $p(t, 0) = \mathbb{P}(\tau > t)$ .  $\square$

**Remark 2.2.** *Not surprisingly, we can also easily handle the case where the barriers move according to a geometric Brownian motion, i.e.*

$$\lambda_t = \sum_{i=1}^n \mu_i \mathbf{1}_{\{C_i e^{(\alpha - \eta^2/2)t + \eta Z_t} \leq V_t < C_{i-1} e^{(\alpha - \eta^2/2)t + \eta Z_t}\}}, \text{ with } \langle W, Z \rangle_t = \rho t.$$

We exclude the trivial case  $\rho = 1$  with  $\eta = \sigma$  and set  $\varsigma = \sqrt{\sigma^2 + \eta^2 - 2\rho\sigma\eta} > 0$  so that  $B_t = (\sigma W_t - \eta Z_t)/\varsigma$  is a standard Brownian motion. Since  $\mathbf{1}_{\{V_t \leq C_i e^{(\alpha - \eta^2/2)t + \eta Z_t}\}} = \mathbf{1}_{\{B_t + \frac{1}{\varsigma}(r - \alpha - (\sigma^2 - \eta^2)/2)t \leq \frac{1}{\varsigma} b_i\}}$ , we get the Laplace transform of  $\mathbb{P}(\tau \leq t)$  by simply taking

$$b = \frac{1}{\varsigma} \log(C/V_0) \text{ and } m = \frac{1}{\varsigma}(r - \alpha - (\sigma^2 - \eta^2)/2)$$

in Theorem 2.1. Said differently, considering geometric Brownian motion barriers does not lead to a richer family of default distributions.



### 3 CDS Pricing

In this section, we briefly recall what a Credit Default Swap is and give its theoretical price under the intensity model (6). We also give straightforward but interesting properties of the CDS spread in function of the different parameters.

Credit Default Swaps are products providing a financial protection against a firm going bankrupt on a given period in exchange of regular payments. Here, we describe a synthetic CDS on a unity notional value starting at time 0, with a maturity  $T$  and a payment grid  $T_0 = 0 < T_1 < \dots < T_p = T$ . Usually, payments occur quarterly. For  $t \in [0, T)$ ,  $\beta(t)$  denotes the index in  $\{1, \dots, p\}$  of the next payment date, i.e. such that  $T_{\beta(t)-1} \leq t < T_{\beta(t)}$ .

If the default happens before  $T$ , the default leg pays the fraction  $LGD$  of the notional that is not recovered (loss given default). For the sake of simplicity, we assume that  $LGD \in [0, 1]$  is deterministic. Since we also consider a constant interest rate  $r > 0$ , the default leg price is then given by

$$DL(0, T) = \mathbb{E}[e^{-r\tau} \mathbf{1}_{\{\tau \leq T\}} LGD] = LGD \left[ e^{-rT} \mathbb{P}(\tau \leq T) + \int_0^T r e^{-ru} \mathbb{P}(\tau \leq u) du \right]. \quad (17)$$

The payment leg consists in regular (time-proportional) payments up to time  $\tau \wedge T$ . This means that they occur until the maturity  $T$  as long as the firm has not defaulted yet. The rate  $R$  of these payments is decided at the beginning of the CDS contract, and the price at time 0 of the payment leg is given by:

$$PL(0, T) = R \times \mathbb{E} \left[ \sum_{i=1}^p (T_i - T_{i-1}) e^{-rT_i} \mathbf{1}_{\{\tau > T_i\}} + (\tau - T_{\beta(\tau)-1}) e^{-r\tau} \mathbf{1}_{\{\tau \leq T\}} \right].$$

By integrating by parts, we get that

$$\begin{aligned} \mathbb{E}[(\tau - T_{\beta(\tau)-1}) e^{-r\tau} \mathbf{1}_{\{\tau \leq T\}}] &= - \int_0^T e^{-ru} (u - T_{\beta(u)-1}) d\mathbb{P}(\tau > u) \\ &= - \sum_{i=1}^p e^{-rT_i} (T_i - T_{i-1}) \mathbb{P}(\tau > T_i) + \int_0^T e^{-ru} \mathbb{P}(\tau > u) du \\ &\quad - \int_0^T r e^{-ru} (u - T_{\beta(u)-1}) \mathbb{P}(\tau > u) du, \end{aligned}$$

and therefore, we obtain that

$$PL(0, T) = R \left[ \int_0^T e^{-ru} \mathbb{P}(\tau > u) du - \int_0^T r e^{-ru} (u - T_{\beta(u)-1}) \mathbb{P}(\tau > u) du \right]. \quad (18)$$

The second term in the bracket can often be neglected in practice, but we have to keep it in our numerical experiments. We also notice that this is the only term depending on the time-grid structure. This is the reason why we do not recall this dependency in our notations for the payment leg which mainly depends on the starting and ending dates.

Up to now<sup>1</sup>, the market practice has been to quote the fair CDS spread  $R(0, T)$  which makes both legs equal:

$$R(0, T) = LGD \frac{e^{-rT} \mathbb{P}(\tau \leq T) + \int_0^T r e^{-ru} \mathbb{P}(\tau \leq u) du}{\int_0^T e^{-ru} \mathbb{P}(\tau > u) du - \int_0^T r e^{-ru} (u - T_{\beta(u)-1}) \mathbb{P}(\tau > u) du}. \quad (19)$$

This rate depends on the default time only through its cumulative distribution function ( $\mathbb{P}(\tau \leq t), t \in [0, T]$ ). In our model, it is denoted by  $P_{\mathbf{b}, m, \boldsymbol{\mu}}(t)$ , and we get the following result.

**Proposition 3.1.** *With a deterministic interest rate  $r > 0$  and a deterministic recovery rate  $1 - LGD \in [0, 1]$ , the CDS price with the intensity model (6) is given by:*

$$R^{\text{model}}(0, T) = LGD \frac{e^{-rT} P_{\mathbf{b}, m, \boldsymbol{\mu}}(T) + \int_0^T r e^{-ru} P_{\mathbf{b}, m, \boldsymbol{\mu}}(u) du}{\int_0^T e^{-ru} P_{\mathbf{b}, m, \boldsymbol{\mu}}^c(u) du - \int_0^T r e^{-ru} (u - T_{\beta(u)-1}) P_{\mathbf{b}, m, \boldsymbol{\mu}}^c(u) du},$$

where  $b = \frac{1}{\sigma} \log(C/V_0)$  and  $m = \frac{1}{\sigma}(r - \alpha - \sigma^2/2)$ . Moreover, if we neglect the second integral in the denominator this rate is nondecreasing with respect to each  $C_i$ ,  $\alpha$  and each  $\mu_i$ . We have also the following bounds:

$$\mu_1 \lesssim \frac{R^{\text{model}}(0, T)}{LGD} \lesssim \mu_n. \quad (20)$$

*Proof.* The monotonicity property is a direct consequence of Proposition A.1. Let us prove (20). From (6), we clearly have  $\mu_1 \leq \lambda_t \leq \mu_n$  for any  $t \geq 0$ . From (3), we have  $P_{\mathbf{b}, m, \boldsymbol{\mu}}^c(t) = \mathbb{E}[e^{-\int_0^t \lambda_s ds}]$  and then:

$$e^{-\mu_n t} \leq P_{\mathbf{b}, m, \boldsymbol{\mu}}^c(t) \leq e^{-\mu_1 t}, \quad 1 - e^{-\mu_1 t} \leq P_{\mathbf{b}, m, \boldsymbol{\mu}}(t) \leq 1 - e^{-\mu_n t}.$$

Plugging these inequalities in (17) and (18), and neglecting  $\int_0^T r e^{-ru} (u - T_{\beta(u)-1}) P_{\mathbf{b}, m, \boldsymbol{\mu}}^c(u) du$  in (18), we get:

$$\begin{aligned} \frac{\mu_1}{r + \mu_1} (1 - e^{-(r+\mu_1)T}) &\leq \frac{DL^{\text{model}}(T)}{LGD} \leq \frac{\mu_n}{r + \mu_n} (1 - e^{-(r+\mu_n)T}), \\ \frac{1}{r + \mu_n} (1 - e^{-(r+\mu_n)T}) &\lesssim PL^{\text{model}}(T) \lesssim \frac{1}{r + \mu_1} (1 - e^{-(r+\mu_1)T}), \end{aligned}$$

which gives (20).  $\square$

**Remark 3.2.** *It is possible to extend the intensity model (6) by adding a deterministic nonnegative shift function  $\varphi(t)$ . Namely, if the default  $\tau$  is defined by (3) and*

$$\lambda_t = \sum_{i=1}^n \mu_i \mathbf{1}_{\{C_i e^{\alpha t} \leq V_t < C_{i-1} e^{\alpha t}\}} + \varphi(t),$$

<sup>1</sup>The ISDA has recommended in early 2009 to switch and to quote CDS through the upfront value  $U(0, T)$  such that  $U(0, T) + PL(0, T) = DL(0, T)$ . The CDS spread  $R$  is then standardized to some specific values. (see [www.cdsmodel.com/information/cds-model](http://www.cdsmodel.com/information/cds-model))

its survival probability satisfies  $\mathbb{P}(\tau > t) = e^{-\int_0^t \varphi(s) ds} P_{\mathbf{b}, m, \boldsymbol{\mu}}^c(t)$  for  $t \geq 0$ . In practice, the function  $\varphi(t)$  can be assumed to be piecewise constant between the CDS maturities. Following the same construction as the one given in [6], this function can be chosen to fit exactly the CDS market curve while the remaining parameters  $(\mathbf{b}, m, \boldsymbol{\mu})$  can be used to calibrate further products.

## 4 Calibration to CDS data with one barrier ( $n = 2$ )

In this section, we want to illustrate how the model presented in this paper can be calibrated to the CDS market data. Here, we focus on the simplest form of the model with only one barrier. The calibration issue with  $n > 2$  is discussed in Section 5. Here, our aim is not to provide the ultimate calibration procedure for the model. This task would require to have a market feedback, and we leave it to practitioners. We have decided instead to make one of the simplest choice, and we minimize the Euclidean distance between the theoretical and market CDS prices. Thus, we want to illustrate on market data picked from the past in which cases the model seems to give a rather good fit.

### 4.1 The Calibration procedure

Now, we want to describe the calibration method we have used in our numerical experiments. We denote by  $T^{(1)} < \dots < T^{(\nu)}$  the maturities of the quoted CDS, and  $R^{\text{market}}(0, T^{(1)}), \dots, R^{\text{market}}(0, T^{(\nu)})$  their market prices. In practice, we have  $\nu = 8$  market data sets for

$$T^{(1)} = 0.5, T^{(2)} = 1, T^{(3)} = 2, T^{(4)} = 3, T^{(5)} = 4, T^{(6)} = 5, T^{(7)} = 7 \text{ and } T^{(8)} = 10 \text{ years,} \quad (21)$$

and quarterly payments. From Theorem 1.1, the default distribution depends on the four parameters  $b, m, \mu_1$  and  $\mu_2$ . Our goal is to minimize the following distance between model and market prices:

$$\min_{b, m \in \mathbb{R}, 0 < \mu_1 < \mu_2} \sum_{i=1}^{\nu} (R^{\text{model}}(0, T^{(i)}) - R^{\text{market}}(0, T^{(i)}))^2. \quad (22)$$

As already mentioned, there are probably better criteria to be minimized according to the market data and the purpose of the calibration. Here, we do not wish to discuss this point, but we rather want to qualitatively show what kind of CDS rate curves  $T \mapsto R^{\text{market}}(0, T)$  the model can fit. That is why we have chosen a very simple criterion to minimize.

To minimize (22), we simply use a gradient algorithm, which is very fast and takes advantage of the closed formula (4) and the Laplace inversion methods presented in Section 6. To do so, we need to compute the CDS prices  $R^{\text{model}}(0, T^{(i)})$  and their derivatives with respect to each parameter  $p \in \{b, m, \mu_1, \mu_2\}$ . In Section 6.2, we have explained in detail how to recover  $P_{b, m, \mu_1, \mu_2}(t)$  on a time-grid from its Laplace transform (4) using the FFT. More precisely, we have used the FFT parameters given by (30) with  $\varepsilon = 10^{-5}$ . Similarly,

we obtain by FFT the derivatives  $\partial_p P_{b,m,\mu_1,\mu_2}(t)$  on the same time-grid. Their Laplace transforms can be obtained by simply differentiating formula (4). However, we have noticed that finite differences can also be used as a good proxy of the derivatives. Then, it is easy to compute the default and payment legs and their sensitivities with respect to each parameter. Numerical integration is performed using Simpson's rule. This is very efficient thanks to the regularity of the cdf (Proposition A.3). Last, we compute CDS prices and their derivatives.

To test this calibration procedure, we have computed CDS prices in our model considering them as Market data, and then we have tried to find back the parameters by minimizing (22). The minimization is really fast and takes very few seconds. Thanks to (20), we start the gradient algorithm from the point

$$b = 0, m = 0, \mu_1 = \min_{i=1,\dots,\nu} R^{\text{market}}(0, T^{(i)})/LGD, \mu_2 = \max_{i=1,\dots,\nu} R^{\text{market}}(0, T^{(i)})/LGD.$$

Unfortunately, it sometimes fails and the gradient algorithm is trapped in local minima. This is partly due to a rather sensitive dependency between the parameters  $b$  and  $m$ . Then, it can be worth starting the gradient algorithm from a point where these parameters are both non zero. However, it is difficult to have a guess on the values of  $b$  and  $m$ . We have used the following way to get a prior on  $(b, m)$ .

- We take a finite set  $\mathcal{S} \subset \mathbb{R}^2$ , typically  $\mathcal{S} = \{-B + 2iB/p, i = 0, \dots, p\} \times \{-M + 2iM/p, i = 0, \dots, p\}$  for some  $B, M > 0, p \in \mathbb{N}^*$ . For  $(b, m) \in \mathcal{S}$ , we minimize the criterion (22) with respect to  $\mu_1$  and  $\mu_2$ , keeping  $b$  and  $m$  constant. In practice, we have mostly taken  $B, M \in \{1, 2\}$  and  $p = 8$ .
- Then, we select the couple  $(b, m) \in \mathcal{S}$  which achieves the smallest score and use it (with the optimized parameters  $\mu_1$  and  $\mu_2$ ) as the initial point of the gradient algorithm for (22).

This procedure generally improves the basic one. However, our minimization problem is ill-posed and significantly different parameters can lead to rather close CDS rates. Let us take the case of a constant intensity model  $\lambda > 0$ , which leads to a flat CDS rate curve from (20). This case corresponds to many different sets of parameters in our model, namely:

1.  $\mu_1 = \mu_2 = \lambda$ , with  $b, \lambda \in \mathbb{R}$  arbitrarily chosen,
2.  $\mu_1 = \lambda, b \rightarrow -\infty$ , with  $m \in \mathbb{R}$  and  $\mu_2 > \mu_1$  arbitrarily chosen,
3.  $\mu_2 = \lambda, b \rightarrow +\infty$ , with  $m \in \mathbb{R}$  and  $\mu_2 > \mu_1$  arbitrarily chosen.

Thus, calibrating very flat CDS spreads can lead to many different satisfactory parameter configurations. We have found other less trivial examples when testing our calibration procedure. In Figure 1, we give two sets of parameters leading to CDS prices which are close up to a 1% relative error but have very similar cdfs. This shows that only calibrating the model to CDS prices, which only depend on the default cdf, may not be sufficient to determine parameters uniquely. Further information on the dependency between the firm value and the default event can be necessary in some cases for that.

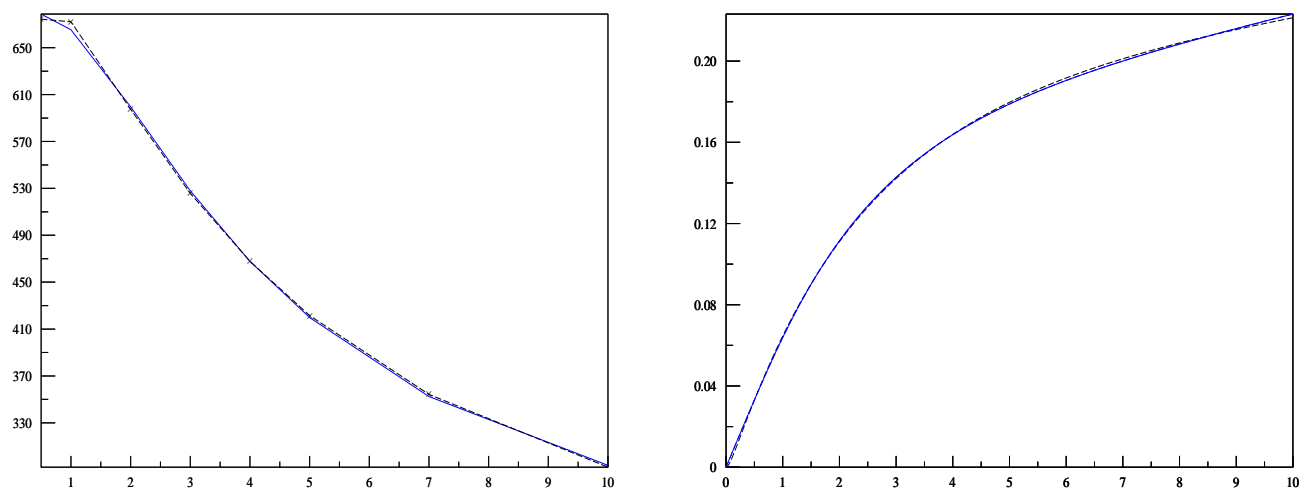


Figure 1: In the l.h.s. picture the CDS prices are plotted as functions of the maturities (21). Prices are given in basis points ( $10^{-4}$ ) with  $LGD = 1$  and  $r = 5\%$ . The r.h.s picture shows the corresponding cumulative distribution functions. The dashed line is obtained with  $b = -0.2$ ,  $m = 0.6$ ,  $\mu_1 = 0.005$  and  $\mu_2 = 0.3$  and the solid line is with  $b = 2.168849$ ,  $m = 0.912237$ ,  $\mu_1 = 0.008414$  and  $\mu_2 = 0.067515$ .

## 4.2 Calibration on Market data

Now, we want to give calibration results under very different CDS rate data. Here, we chose to calibrate all the four parameters  $(b, m, \mu_1, \mu_2)$  to check if they are sufficient to fit the market data well. However, some of these parameters have an economic meaning. For example, the firm value can be related to its balance sheet and any other relevant information available in practice. In that case, one would like to fix some parameters or restrict them to lie in some interval. Here, for the sake of simplicity, we only consider the information given by the CDS prices and leave a more elaborated calibration for further research.

We have picked up very different examples from 2006 to 2009 on Crédit Agricole (bank, CA in short), PSA, Ford (car companies) and Saint-Gobain (glass maker, SG in short). In all our examples, we have set  $LGD = 0.6$ , except for Crédit Agricole for which we have taken  $LGD = 0.8$  as it is commonly done for bank companies. We have also taken  $r = 5\%$  for the sake of simplicity, since  $r$  has anyway a rather minor impact on the CDS spread values. The maturities observed on the market are the one listed in (21). In all the figures, we have plotted in dotted lines the CDS market data and in solid lines the CDS prices obtained with the calibrated model. Prices are given in basis points ( $10^{-4}$ ). For each example, we give the calibrated parameters  $(b, m, \mu_1, \mu_2)$ . To interpret them into the original firm value framework, we have also indicated the corresponding values of  $V_0/C = e^{-b\sigma}$  and  $\alpha = r - \sigma m - \sigma^2/2$ , taking the one-year at-the-money implied volatility as a proxy of the firm value volatility. However, as pointed in Section 4.1, significantly different parameters can lead to analogous CDS prices. The calibration to CDS prices only allows to fit the default cdf. This is why we have added in each case a subplot of the calibrated cdf,  $(P_{b,m,\mu_1,\mu_2}(t), t \in [0, T^{(8)}])$ .

We have split the results into three classes.

- The curve  $T \mapsto R^{\text{market}}(0, T)$  is mostly increasing. Roughly speaking, it happens when the firm's future is more unsure than its present.
- The curve  $T \mapsto R^{\text{market}}(0, T)$  is mostly decreasing. This usually means that the firm is in a critical period. If it overcomes this time, its future will be less risky.
- Most of the market data correspond to the two previous cases. However, when a firm switches from one regime to the other, the CDS curve tends to be flat, keeping often however a gentle slope.

### 4.2.1 Increasing CDS spreads

We start with data prior to the subprime crisis on companies presenting a low risk profile. Their calibration are plotted in Figure 2. Not surprisingly, in this case the model is able to fit the prices well, with a relative error of a few percents. As one could expect, the firm value starts in both cases above the threshold  $C$  in the “ $\mu_2$  region” and is drifted to the “ $\mu_1$  region” since the parameter  $m$  is negative (or equivalently,  $\alpha > r - \sigma^2/2$ ).

We have also considered increasing patterns with a higher level of risk, and the calibrating results are drawn in Figure 3. The Ford curve (left) is really well fitted. The

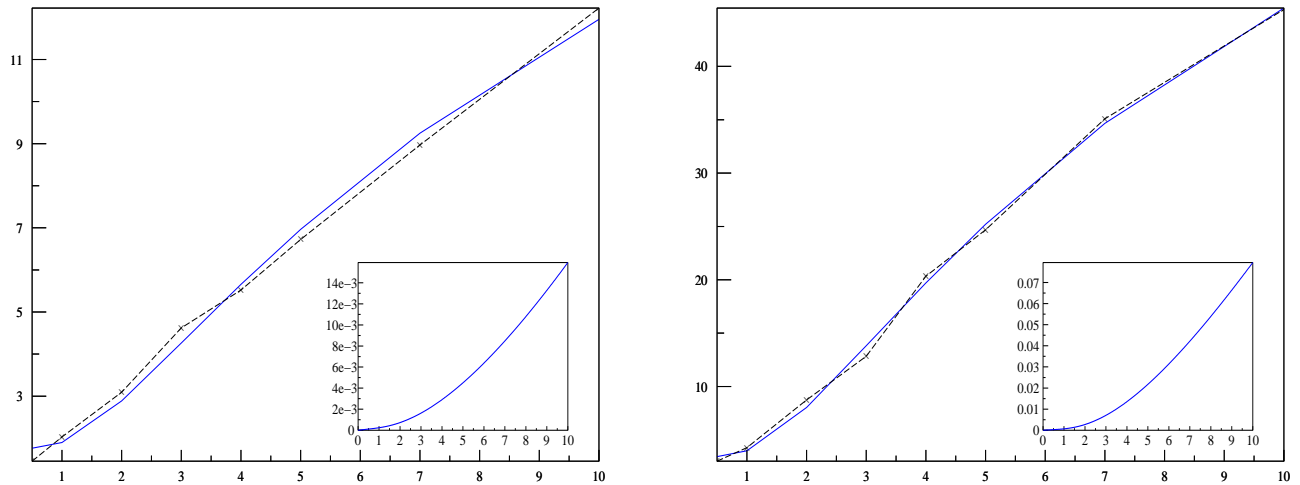


Figure 2: *Left, CA 08/31/06:*  $b = -2.3415$ ,  $m = -0.2172$ ,  $\mu_1 = 2.164 \times 10^{-4}$ ,  $\mu_2 = 5.597 \times 10^{-3}$ ,  $V_0/C = 1.753$ ,  $\alpha = -1.78 \times 10^{-2}$ . *Right, PSA 05/03/06:*  $b = -2.3878$ ,  $m = -0.3745$ ,  $\mu_1 = 5.581 \times 10^{-4}$ ,  $\mu_2 = 2.214 \times 10^{-2}$ ,  $V_0/C = 1.757$ ,  $\alpha = 2.038 \times 10^{-2}$ .

Saint-Gobain rates (left) are globally well captured, but some irregularities are smoothed by the calibrated curve. Once again, the firm value starts above the threshold in the safer side, which confirms the heuristic interpretation made above on increasing CDS curves.

#### 4.2.2 Decreasing CDS spreads

Now, we want to test if the model is also able to fit decreasing CDS curves. As already mentioned, it happens when a firm goes through a difficult period. We give in Figure 4 two stressed examples on Ford company, taken at the climax of its crisis in November 2008 (left) and in February 2009 (right). Both curves are correctly fitted. The most significant relative difference between market and model prices is equal to 6% on November data and 2% on February data. As expected, in both cases, the firm value starts below the threshold in the “ $\mu_2$  region” and goes gradually to the “ $\mu_1$  region” since  $m > 0$  (or equivalently,  $\alpha < r - \sigma^2/2$ ).

Now, we want to test the model on decreasing but less stressed patterns. We also want to see if it can in addition fit an initial bump. Indeed, it happens quite often on decreasing curves that the 6-month rate is however lower than the one-year rate. Roughly speaking, this means that the firm is in difficulty but the market however believes that it has some guarantee to live in the very short future. We have drawn in Figure 5 two examples on PSA (left) and Saint-Gobain (right). In the first case, the model does not seem able to replicate the initial bump, but the remaining part of the curve is well fitted. The bump is approximated by a flat curve in between. Doing this, the gradient algorithm explores

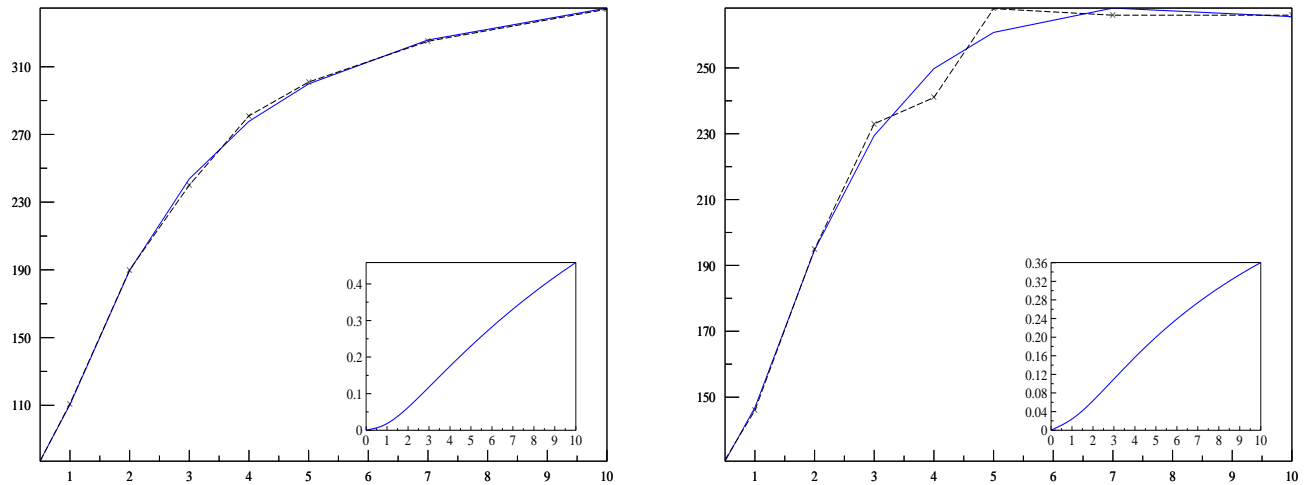


Figure 3: *Left, Ford 11/30/06:*  $b = -1.734$ ,  $m = -1.363$ ,  $\mu_1 = 1.2 \times 10^{-2}$ ,  $\mu_2 = 7.05 \times 10^{-2}$ ,  $V_0/C = 2.173$ ,  $\alpha = 0.436$ . *Right, SG 10/08/08:*  $b = -1.897$ ,  $m = 0.1725$ ,  $\mu_1 = 2.135 \times 10^{-2}$ ,  $\mu_2 = 0.652$ ,  $V_0/C = 2.8506$ ,  $\alpha = -0.3213$ .

rather large and unrealistic parameters for  $b$  and  $m$ . Instead, on the Saint-Gobain example, the whole shape is well fitted with very rational parameters.

### 4.2.3 Almost flat CDS spreads

Last, we give two examples of rather flat CDS rate curves. This kind of pattern is more uncommon and is observed in particular when a firm switches from an increasing to a decreasing curve like Saint-Gobain between 10/08/08 (Fig. 3) and 12/01/08 (Fig. 5). Flat curves are a priori not very difficult to fit since a constant intensity model can already give a first possible approximation. We show in Figure 6 the transition made by the Saint-Gobain curve. On these flat shapes, the fitting is really good and the relative error on prices does not exceed 1%.

Let us draw a short conclusion on these calibration results. The model is able to fit a wide range of CDS data, from a very low risk level (Fig. 2) to highly stressed spreads (Fig. 4) as well as intermediate settings (Fig. 3, 5, 6) that are more frequently observed. Of course, not all the prices are perfectly matched, but the spread curves are globally well captured. Concerning the meaning of the parameters, one has to be careful since only calibrating to the CDS rates is a priori not enough to determine them (see Fig. 1). However, at least in the extreme settings, the values of  $V_0/C$  and  $\alpha$  which we have obtained are as expected greater (resp. lower) than 1 and  $r - \sigma^2/2$  in Fig. 2 (resp. Fig. 4), which means that the firm value gradually shifts from the  $\mu_1$  (resp.  $\mu_2$ ) to the  $\mu_2$  (resp.  $\mu_1$ ) area.



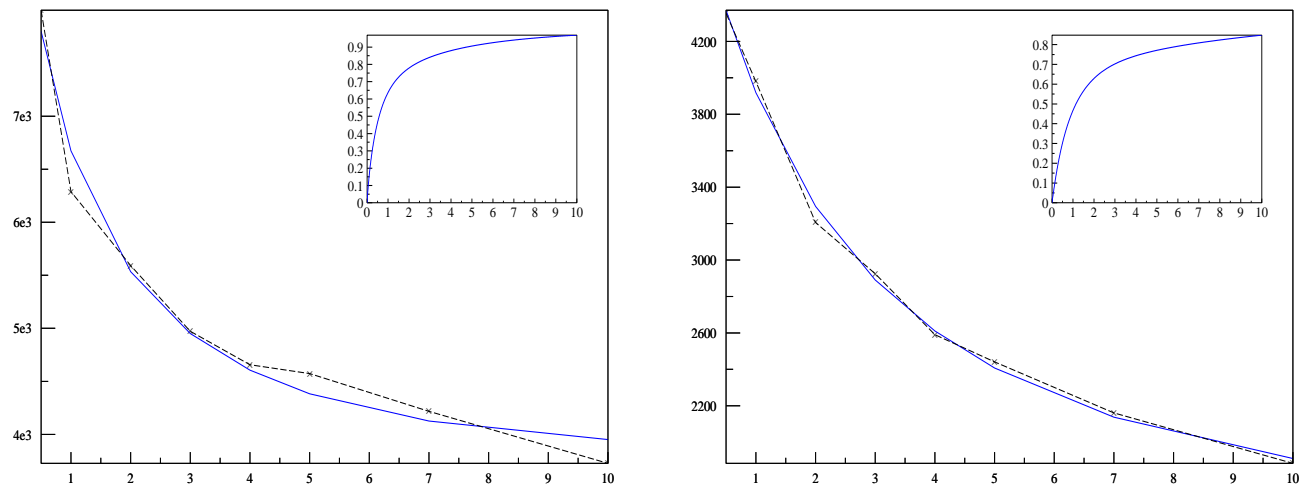


Figure 4: *Left, Ford 11/24/08:*  $b = 0.209$ ,  $m = 0.344$ ,  $\mu_1 = 0.2014$ ,  $\mu_2 = 1.986$ ,  $V_0/C = 0.716$ ,  $\alpha = -1.3$ . *Right, Ford 02/25/09:*  $b = 0.8517$ ,  $m = 0.5277$ ,  $\mu_1 = 6.85 \times 10^{-2}$ ,  $\mu_2 = 0.7806$ ,  $V_0/C = 0.3355$ ,  $\alpha = -1.2676$

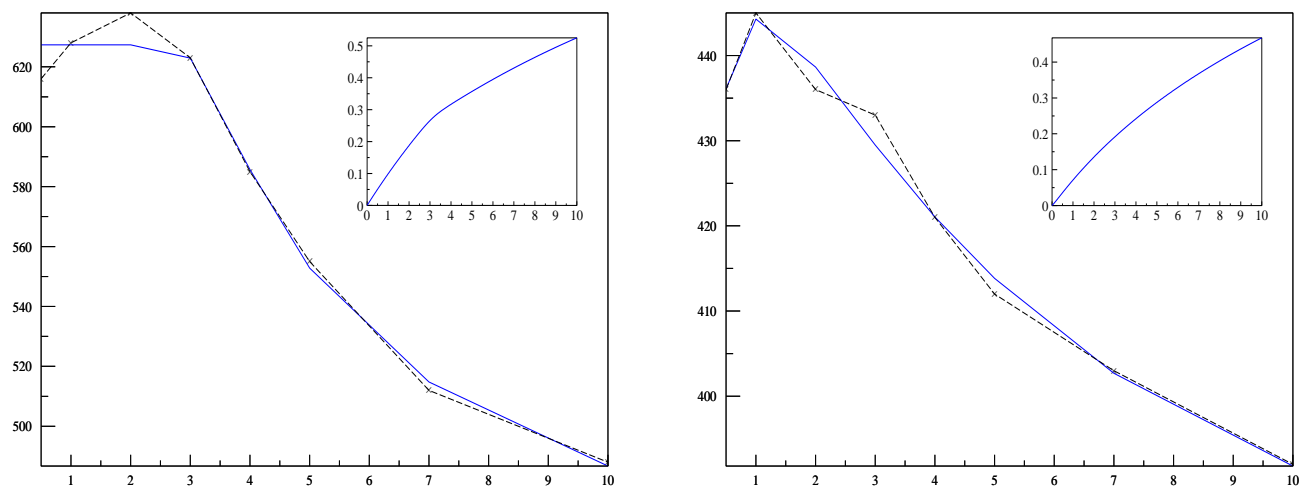


Figure 5: *Left, PSA 03/06/09:*  $b = 15.55$ ,  $m = 4.889$ ,  $\mu_1 = 6.055 \times 10^{-2}$ ,  $\mu_2 = 0.104$ ,  $V_0/C = 6.32 \times 10^{-5}$ ,  $\alpha = -3.3$ . *Right, SG 12/01/08:*  $b = -0.268$ ,  $m = 0.567$ ,  $\mu_1 = 5.46 \times 10^{-2}$ ,  $\mu_2 = 0.154$ ,  $V_0/C = 1.1837$ ,  $\alpha = -0.6213$ .

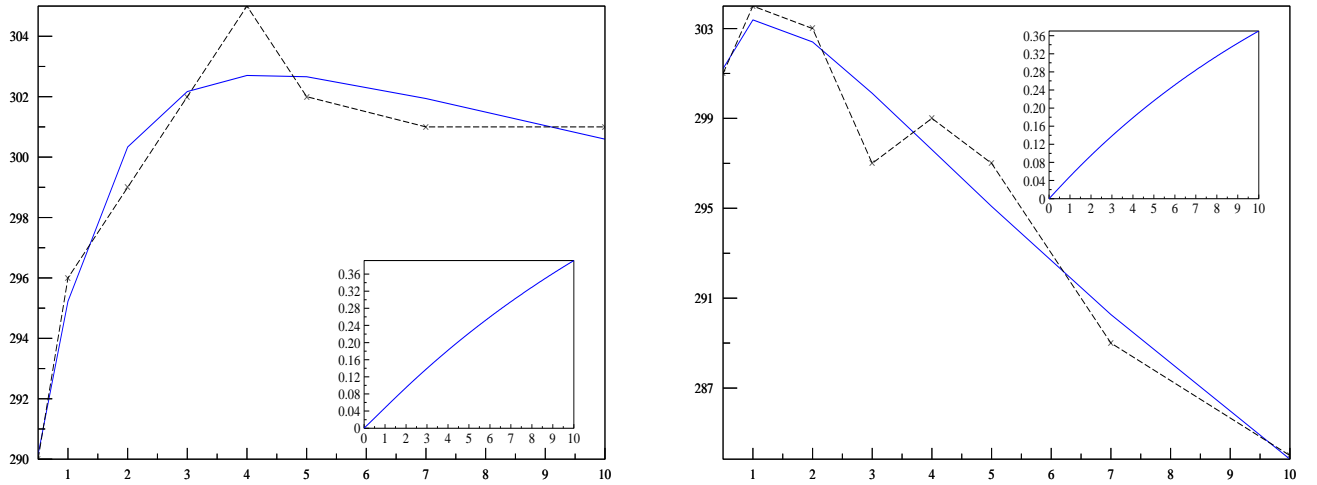


Figure 6: *Left, SG 10/21/08:*  $b = -1.032$ ,  $m = 0.493$ ,  $\mu_1 = 4.75 \times 10^{-2}$ ,  $\mu_2 = 9.23 \times 10^{-2}$ ,  $V_0/C = 1.83$ ,  $\alpha = -0.531$ . *Right, SG 10/31/08:*  $b = -3.42 \times 10^{-2}$ ,  $m = 4.69 \times 10^{-2}$ ,  $\mu_1 = 1.45 \times 10^{-2}$ ,  $\mu_2 = 9.295 \times 10^{-2}$ ,  $V_0/C = 1.021$ ,  $\alpha = -0.282$ .

## 5 Calibration with multiple barriers ( $n \geq 3$ )

In the previous section, we have only considered the calibration with one barrier. We have noticed that the model already fits the market well in that case for a rather wide range of data. Here, we want to discuss the calibration of the full model. The default distribution is parametrized by  $2n$  parameters ( $m, b_1, \dots, b_{n-1}$  and  $\mu_1, \dots, \mu_n$ ).

A first natural idea would be to find implicit parameters. Thus, CDS market data could be expressed as an implicit function that gives the intensity as a function of the firm value. For example, we could fix  $\mu_1, \dots, \mu_n$  to some standard values corresponding to credit grades and look for parameters  $m, b_1, \dots, b_{n-1}$  which exactly fit the CDS market data. However, it is not possible in general to get an implicit curve like this. We explain why by giving a heuristic argument. From (8), we can see that the default intensity will basically increase (resp. decrease) when  $m < 0$  (resp  $m > 0$ ). Thanks to the Brownian diffusion, this global trend can be moderated. For example, if we consider the case with one negative barrier and  $m > 0$ , the default intensity can increase for short maturities because the diffusion part enables to explore the riskiest region at the beginning. This is what happens in the right hand side example of Figure 5 and gives a bump shape for CDS spreads. However, not all kinds of CDS shapes can be obtained with the intensity model (6). In Figure 7, we have plotted the deterministic piecewise default intensity which exactly matches CDS data for PSA in March 2009. We observe that it is nondecreasing up to 2 years, nonincreasing between 2Y and 7Y, and again nondecreasing on the last period. Typically, the model (6) cannot reproduce this kind of alternate profile and can only capture a global trend. Thus,

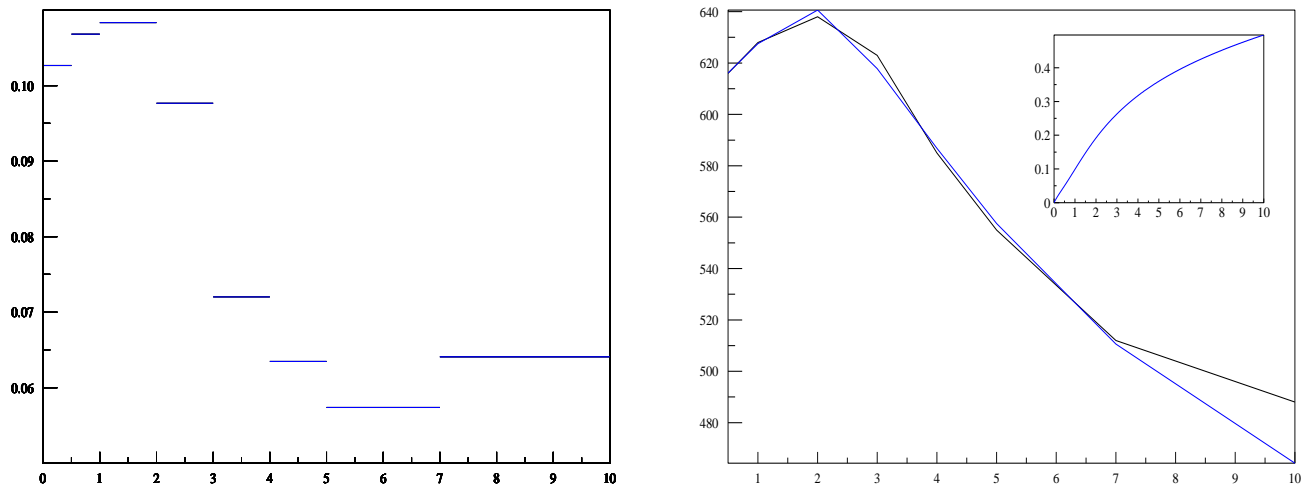


Figure 7: PSA 03/06/09: *Left*: piecewise constant deterministic intensity function that exactly fits CDS spreads data. *Right*: calibration with  $n = 3$  of CDS spreads up to maturity 7Y:  $m = 0.4$ ,  $b_1 = 0.5$ ,  $b_2 = -1.5$ ,  $\mu_1 = 3.398 \times 10^{-2}$ ,  $\mu_2 = 0.11417$  and  $\mu_3 = 1.917$ .

we cannot get an implicit curve for these kinds of CDS data for which the default risk swings along the time.

Since it is not possible to find implicit parameters, we now want to discuss the possibility to calibrate several barriers. Calibrating more than one barrier is not really easy in practice. First of all, we have observed that the calibration with one barrier was already ill-posed (see Figure 1) because two different sets of parameters can lead to the same distribution function. Obviously, this will not improve when adding parameters. The second reason is that, beyond the meaning of the calibrated parameters, the calibration with only one barrier in Section 4 was already rather satisfying and it is in practice rather difficult to get a significantly better fit of CDS data with two or more barriers. This is why we have mainly focused on an example where the calibration with only one barrier is not fully satisfying. Namely, we have again considered the data of PSA in March 2009. Even if CDS data are reasonably fitted, the calibrated parameters in 5 are rather stressed  $b \approx 15$  and  $m \approx 5$ , which makes the diffusion part rather negligible. Roughly speaking, the intensity is mainly equal to  $\mu_2$  before 3Y and to  $\mu_1$  after 3Y from Equation (8) and somehow, the calibrated model is not really far from a deterministic intensity model. Thus, it does not really depend on the firm value. A possible reason of the difficulty to fit these data could be the alternate shape of the calibrated piecewise intensity in Figure (7) which cannot be captured by our model as it has already been mentioned before. To correct this drawback, it is possible in practice to add a deterministic shift as suggested in Remark 3.2. However, for the sake of simplicity, we have instead decided to ignore the 10Y CDS data and minimize the cost function (22) with  $\nu = 7$ . Doing so, we have not been able to significantly improve the

calibration obtained in Figure 5 with one barrier. Instead, we have been able to fit rather well the CDS data up to 7Y by adding a second barrier as given in Figure 7. In particular, the initial bump is particularly well fitted. We also observe that it was useful to remove the 10Y data from the calibration. The calibrated parameters have been obtained by using some heuristic arguments on the expected time spent below a barrier. Explaining the details would lead to a rather tedious discussion which we prefer to skip.

To conclude this section, we would like to stress that calibrating with more than one barrier is difficult and in general does not significantly improve the fit to CDS data. Even though in some cases we get a better fit by adding one barrier, the calibrated parameters are also not so meaningful since we only have 8 data. However, the model with many barriers can be interesting to fit other possible liquid products like options on CDS.

## 6 Numerical methods for Laplace inversion

From Theorem 1.1, we know that the default time distribution is tractable using the semi-analytical formula for its Laplace transform. In this section, we are investigating different ways of inverting this Laplace transform to recover the cumulative distribution function of the default time  $\tau$ , and also its first order derivatives with respect to each parameter. Recovering these derivatives enables us to quickly compute the sensitivities with respect to the different parameters, which is of a great importance for the calibration procedure, if one wants to use a gradient algorithm to minimize some distance between the real and theoretical prices.

In this section,  $f : \mathbb{R} \rightarrow \mathbb{R}$  is a real valued function vanishing on  $\mathbb{R}_-$  and such that  $f(t)e^{-\gamma t}$  is integrable for some  $\gamma > 0$ . We will denote by  $\hat{f}(z) = \int_0^\infty e^{-zt} f(t) dt$  its Laplace transform for  $z \in \mathbb{C}$  when the integral is well-defined, i.e at least when  $\mathcal{R}e(z) \geq \gamma$ . The scope of this section is to present numerical methods to recover  $f$  from  $\hat{f}$  and analyze their accuracies. Basically in our model,  $f$  will be either  $\mathbb{P}(\tau \leq t)$  or its derivative w.r.t. one of the model parameters.

### 6.1 The Fourier series approximation

From the formulas obtained for the Laplace transform of the default time, it is clear that these Laplace transforms are analytical in the complex half-plane  $\mathbb{C}_+$ . Thanks to [18], we know how to recover a function from its Laplace transform.

**Theorem 6.1.** *Let  $f$  be a continuous function defined on  $\mathbb{R}_+$  and  $\gamma$  a positive number. If the function  $f(t)e^{-\gamma t}$  is integrable, then its Laplace transform  $\hat{f}(z) = \int_0^\infty e^{-zt} f(t) dt$  is well defined on  $\{z \in \mathbb{C}, \mathcal{R}e(z) \geq \gamma\}$ , and  $f$  can be recovered from the contour integral*

$$f(t) = \frac{1}{2\pi i} \int_{\gamma-i\infty}^{\gamma+i\infty} e^{st} \hat{f}(s) ds = \frac{e^{\gamma t}}{2\pi} \int_{-\infty}^{+\infty} e^{-ist} \hat{f}(\gamma - is) ds, \quad t > 0. \quad (23)$$

For any real valued function satisfying the hypotheses of Theorem 6.1, we introduce the following discretisation of Equation (23) with step  $h > 0$

$$f_h(t) = \frac{h e^{\gamma t}}{2\pi} \sum_{k=-\infty}^{\infty} e^{-ikh t} \hat{f}(\gamma - ikh). \quad (24)$$

From [1, Theorem 5], one can prove using the Poisson summation formula that

**Proposition 6.2.** *If  $f$  is a continuous bounded function satisfying  $f(t) = 0$  for  $t < 0$ , we have*

$$\forall t < 2\pi/h, |f(t) - f_h(t)| \leq \|f\|_{\infty} \frac{e^{-2\pi\gamma/h}}{1 - e^{-2\pi\gamma/h}}. \quad (25)$$

## 6.2 The fast Fourier transform approach

In this section, we focus on the inversion using an FFT based algorithm. First, let us recall that for a given integer  $N \in \mathbb{N}^*$ , the forward discrete Fourier transform (DFT) of  $(x_k, k = 0, \dots, N-1)$  is defined by

$$\hat{x}_l = \sum_{k=0}^{N-1} e^{-2i\pi kl/N} x_k, \quad \text{for } l = 0, \dots, N-1.$$

It is well known that there are Fast Fourier Transform algorithms to compute  $(\hat{x}_l, l = 0, \dots, N-1)$  with a time complexity proportional to  $N \log(N)$ . In their pathbreaking paper, Cooley and Tukey [12] have given such an algorithm for the special case where  $N$  is a power of 2. Many improvements of this algorithm have been proposed in the literature relaxing this constraint on  $N$ . In finance, the use of the FFT for option pricing has been popularized by Carr and Madan [9]. Here, we use the FFT algorithm in a different manner to compute the cdf of  $\tau$  and its derivatives with respect to each parameter up to some time  $T > 0$ .

Let us assume that we want to recover the function  $f$  on the interval  $[0, T]$ . Typically,  $T$  will represent the largest maturity of the CDS that one wishes to consider. We set  $h < 2\pi/T$ , so that  $h < 2\pi/t$  for any  $t \in (0, T]$  and we can therefore control the error between the Fourier series  $f_h$  and  $f$  thanks to Proposition 6.2:

$$\forall t \in (0, T], |f(t) - f_h(t)| \leq \|f\|_{\infty} \frac{e^{-2\pi\gamma/h}}{1 - e^{-2\pi\gamma/h}}.$$

Since  $f$  is real valued,  $\hat{f}(\bar{z}) = \overline{\hat{f}(z)}$ , and we obtain

$$f_h(t) = \frac{h e^{\gamma t}}{2\pi} \hat{f}(\gamma) + \frac{h e^{\gamma t}}{\pi} \operatorname{Re} \left( \sum_{k=1}^{\infty} e^{-ikh t} \hat{f}(\gamma - ikh) \right), \quad (26)$$

which can be approximated by the following finite sum

$$f_h^N(t) = \frac{h e^{\gamma t}}{2\pi} \hat{f}(\gamma) + \frac{h e^{\gamma t}}{\pi} \operatorname{Re} \left( \sum_{k=1}^N e^{-ikh t} \hat{f}(\gamma - ikh) \right). \quad (27)$$

For  $1 \leq l \leq N$ , we set  $t_l = 2\pi l / (Nh)$  to get

$$\begin{aligned} f_h^N(t_l) &= \frac{h e^{\gamma t_l}}{2\pi} \hat{f}(\gamma) + \frac{h e^{\gamma t_l}}{\pi} \operatorname{Re} \left( \sum_{k=1}^N e^{-2i\pi k l / N} \hat{f}(\gamma - ikh) \right) \\ &= \frac{h e^{\gamma t_l}}{2\pi} \hat{f}(\gamma) + \frac{h e^{\gamma t_l}}{\pi} \operatorname{Re} \left( e^{-2i\pi(l-1)/N} \sum_{k=1}^N e^{-2i\pi(k-1)(l-1)/N} e^{-2i\pi k / N} \hat{f}(\gamma - ikh) \right). \end{aligned}$$

Therefore,  $(f_h^N(t_l), l = 1, \dots, N)$  can be computed easily using the direct FFT algorithm on the vector  $(e^{-2ik\pi/N} \hat{f}(\gamma - ikh), k = 1, \dots, N)$ .

Now, let us analyze the error induced by approximating  $(f(t_l))_l$  by  $(f_h^N(t_l))_l$ . The following proposition gives an upper bound of the error involved in the truncation of the series appearing in  $f_h$ .

**Proposition 6.3.** *Let  $f$  be a function of class  $\mathcal{C}^3$  on  $\mathbb{R}_+$  such that there exists  $\epsilon > 0$  satisfying  $\forall k \leq 3$ ,  $f^{(k)}(s) = \mathcal{O}(e^{(\gamma-\epsilon)s})$ . Let us assume moreover that  $f(0) = 0$ . Let  $A \in (0, 2\pi)$ . Then, there exists a constant  $K > 0$  independent of  $t$  such that:*

$$\forall t \in (0, A/h], |f_h^N(t) - f_h(t)| \leq K(1 + 1/t) \frac{e^{\gamma t}}{N^2}. \quad (28)$$

*Proof.* From three successive integrations by parts, we get:

$$\begin{aligned} \hat{f}(\gamma - ikh) &= \int_0^\infty e^{(ikh-\gamma)u} f(u) du \\ &= \frac{-f'(0)}{(ikh-\gamma)^2} + \frac{f''(0)}{(ikh-\gamma)^3} - \int_0^\infty \frac{f^{(3)}(u)}{(ikh-\gamma)^3} e^{(ikh-\gamma)u} du. \end{aligned}$$

We set  $E_k = \sum_{j=0}^{k-1} e^{-ijht} = (1 - e^{-ikh t}) / (1 - e^{-iht})$  and get by a summation by parts

$$\sum_{k=0}^N \frac{e^{-ikh t}}{(ikh-\gamma)^2} = \frac{E_{N+1}}{(iNh-\gamma)^2} + \sum_{k=1}^N E_k \frac{h(2\gamma + i(2k-1)h)}{(ikh-\gamma)^2(i(k-1)h-\gamma)^2} - \frac{1}{\gamma^2}.$$

Therefore, we deduce that:

$$\begin{aligned} \frac{2\pi}{h e^{\gamma t}} (f_h^N(t) - f_h(t)) &= 2f'(0) \operatorname{Re} \left( \frac{E_{N+1}}{(iNh-\gamma)^2} + \sum_{k=N+1}^\infty E_k \frac{h(2\gamma + i(2k-1)h)}{(ikh-\gamma)^2(i(k-1)h-\gamma)^2} \right) \\ &\quad + 2 \operatorname{Re} \left( \sum_{k=N+1}^\infty e^{-ikh t} \frac{f''(0) - \int_0^\infty f^{(3)}(u) e^{(-\gamma+ikh)u} du}{(ikh-\gamma)^3} du \right). \end{aligned}$$

Then, using that for any  $k \in \mathbb{N}$   $|E_k| \leq 2/|1 - e^{-iht}|$ , we get:

$$\begin{aligned} \left| \frac{2\pi}{he^{\gamma t}} (f_h^N(t) - f_h(t)) \right| &\leq \frac{4|f'(0)|}{|1 - e^{-iht}|} \left( \frac{1}{\gamma^2 + (Nh)^2} + \sum_{k=N+1}^{\infty} h \frac{\sqrt{(2\gamma)^2 + ((2k-1)h)^2}}{(\gamma^2 + (kh)^2)(\gamma^2 + ((k-1)h)^2)} \right) \\ &\quad + 2(|f''(0)| + C/\epsilon) \sum_{k=N+1}^{\infty} \frac{1}{(\gamma^2 + (kh)^2)^{3/2}}, \end{aligned}$$

where  $C = \sup_{t \geq 0} |f^{(3)}(t) e^{(\epsilon-\gamma)t}|$ . The result follows from noticing that  $\sup_{y \in [0, A]} \frac{y}{|1 - e^{-iy}|} < \infty$ .  $\square$

**Corollary 6.4.** *Let  $f$  be a bounded function of class  $\mathcal{C}^3$  on  $\mathbb{R}_+$  such that there exists  $\epsilon > 0$  satisfying  $\forall k \leq 3$ ,  $f^{(k)}(s) = \mathcal{O}(e^{(\gamma-\epsilon)s})$ . Let  $A \in (0, 2\pi)$  and  $h \leq A/T$ .*

*Then, there exists a constant  $K > 0$  such that*

$$\forall l \geq 1, t_l \leq T, |f_h^N(t_l) - f(t_l)| \leq K \max \left( \frac{e^{\gamma T}}{N^2}, \frac{h}{2\pi N} \right) + \|f\|_{\infty} \frac{e^{-2\pi\gamma/h}}{1 - e^{-2\pi\gamma/h}}.$$

*Proof.* It is sufficient to use Propositions 6.2 and 6.3, and to notice that  $\max_{t \in [t_1, T]} (e^{\gamma t} / t) \leq \max(e^{\gamma t_1} / t_1, e^{\gamma T} / T)$ .  $\square$

**Remark 6.5.** *When there is only one barrier ( $n = 2$ ) the results obtained in Appendix A.2 enable to check the regularity needed in the above corollary to compute the cumulative distribution function of the default time.*

*When  $b \neq 0$ , the functions  $P_{b,m,\mu_1,\mu_2}(t)$  and  $\partial_p P_{b,m,\mu_1,\mu_2}(t)$  for  $p \in \{b, m, \mu_1, \mu_2\}$  satisfy the above assumption thanks to Proposition A.3.*

*When  $b = 0$ , we can check from (4) that there exist some constants  $c$  and  $c_p$  for  $p \in \{m, \mu_1, \mu_2\}$  such that the following expansions hold when  $k \rightarrow +\infty$ :*

$$L_{0,m,\mu_1,\mu_2}(\gamma - ikh) = \frac{c}{(\gamma - ikh)^2} + \mathcal{O}(1/k^3), \quad \text{and} \quad \partial_p L_{0,m,\mu_1,\mu_2}(\gamma - ikh) = \frac{c_p}{(\gamma - ikh)^2} + \mathcal{O}(1/k^3).$$

*Therefore, we can use the same proof as in Proposition 6.3 to bound the truncation error by  $K(1+1/t)\frac{e^{\gamma t}}{N^2}$ . On the contrary, the derivative with respect to  $b$  satisfies  $\partial_b L_{0,m,\mu_1,\mu_2}(\gamma - ikh) = (m + \sqrt{2(\gamma - ikh + \mu_1) + m^2})L_{0,m,\mu_1,\mu_2}(\gamma - ikh) = \frac{c_b}{(\gamma - ikh)^{3/2}} + \mathcal{O}(1/k^{5/2})$ . Thus, the same proof only gives a truncation error bounded by  $K(1+1/t)\frac{e^{\gamma t}}{N^{3/2}}$  in this case, which however still goes to zero when  $N$  is large enough.*

### 6.3 Practical implementation in our model.

Now, let us explain how to choose the parameters in our model in order to achieve an accuracy of order  $\epsilon > 0$ . We start with the one barrier case ( $n = 2$ ) for which we can take  $\gamma > 0$  as close to 0 as we wish thanks to Proposition A.3. The following conditions

$$h < 2\pi/T, \quad \frac{2\pi\gamma}{h} = \log(1 + 1/\epsilon), \quad N > \max \left( \frac{h}{2\pi\epsilon}, \sqrt{\frac{e^{\gamma T}}{\epsilon}} \right) \quad (29)$$

ensure by Corollary 6.4 that  $\sup_{l \geq 1, t_l \leq T} |f_h^N(t_l) - f(t_l)|$  is of order  $\varepsilon$ .

In practice, it is important to make the time grid  $(t_l, l = 1 \dots N)$  on which we recover the cdf (and its derivatives) coincide with the payment dates of all the products considered. Typically, this grid should encompass the quarterly time grid to easily compute the CDS prices and their sensitivities. More precisely, we will compute the integrals defining default and payment leg prices in (17) and (18) using the Simpson rule, which is very efficient since the integrated functions are regular enough (namely  $\mathcal{C}^4$ ) as stated by Proposition A.3. To do so, we need a time grid at least twice thinner than the payment grid, and therefore  $1/8$  has to be a multiple of  $t_1 = \frac{2\pi}{Nh}$ . Since in this paper we consider CDS up to  $T = 10$  years, we make the following choice when considering only one barrier ( $n = 2$ ):

$$T = 10, \quad h = \frac{5\pi}{8T}, \quad \gamma = \frac{h}{2\pi} \log(1 + 1/\varepsilon), \quad N = \max \left( 2^{\left\lceil \log_2 \left( \max \left( \frac{h}{2\pi\varepsilon}, \sqrt{\frac{e\gamma T}{\varepsilon}} \right) \right) \right\rceil}, 2^7 \right). \quad (30)$$

This choice automatically guarantees the latter condition:  $1/8$  is clearly a multiple of  $t_1 = 16/N$ .

When considering more than one barrier, we no longer have theoretical results on the time regularity of the cdf of the default time like the one obtained in Appendix A.2. However, the numerical procedure still works. From our numerical experiments, we have noticed that it is wise to decrease  $h$ , especially when  $b_1$  or  $b_{n-1}$  are far away from 0. In that case we have used the following parameters:

$$T = 10, \quad h = \frac{5\pi}{32T}, \quad \gamma = \frac{h}{2\pi} \log(1 + 1/\varepsilon), \quad N = \max \left( 2^{\left\lceil \log_2 \left( \max \left( \frac{h}{2\pi\varepsilon}, \sqrt{\frac{e\gamma T}{\varepsilon}} \right) \right) \right\rceil}, 2^9 \right). \quad (31)$$

## 6.4 The Euler summation

The Laplace inversion based on the FFT is very efficient and enables to very quickly compute the cdf and its derivatives on the whole time interval. However, the time grid has to be regular, which may be a possible drawback when dealing with bespoke products that have unusual payment dates. Here, we present another method to recover the function  $f$  from its Laplace transform at a given time  $t \geq 0$ .

Unlike the FFT approach, we can here choose  $h$  as a function of  $t$ , and the trick consists in choosing  $h = \pi/t$  to get an alternating series in (26):

$$f_{\pi/t}(t) = \frac{e^{\gamma t}}{2t} \widehat{f}(\gamma) + \frac{e^{\gamma t}}{t} \sum_{k=1}^{\infty} (-1)^k \mathcal{R}e \left( \widehat{f} \left( \gamma + i \frac{k\pi}{t} \right) \right). \quad (32)$$

Rather than simply truncating the series like in the FFT algorithm, we use the Euler summation technique as described by [1], which consists in computing the binomial average of  $q$  terms from the  $N$ -th term of the series appearing in (32). The following proposition describes the convergence rate of the binomial average to the infinite series  $f_{\pi/t}(t)$  when  $p$  goes to  $\infty$ . Its proof can be found in Labart and Lelong [15].



**Proposition 6.6.** *Let  $q \in \mathbb{N}^*$  and  $f$  be a function of class  $\mathcal{C}^{q+4}$  such that there exists  $\epsilon > 0$  satisfying  $\forall k \leq q+4$ ,  $f^{(k)}(s) = \mathcal{O}(e^{(\gamma-\epsilon)s})$ . We consider the truncation of the series in (32)*

$$f_{\pi/t}^N(t) = \frac{e^{\gamma t}}{2t} \widehat{f}(\gamma) + \frac{e^{\gamma t}}{t} \sum_{k=1}^N (-1)^k \mathcal{R}e \left( \widehat{f} \left( \gamma + i \frac{\pi k}{t} \right) \right),$$

and  $E(q, N, t) = \sum_{k=0}^q \binom{q}{k} 2^{-q} f_{\pi/t}^{N+k}(t)$ . Then,

$$|f_{\pi/t}(t) - E(q, N, t)| \leq \frac{t e^{\gamma t} |f'(0) - \gamma f(0)|}{\pi^2} \frac{N! (q+1)!}{2^q (N+q+2)!} + \mathcal{O} \left( \frac{1}{N^{q+3}} \right)$$

when  $N$  goes to infinity.

In practice, for  $q = N = 15$  and  $\gamma = 11.5/t$ , we have  $e^{\gamma t} \frac{N! (q+1)!}{2^q (N+q+2)!} \approx 3.13 \times 10^{-10}$ , and it is therefore sufficient to make the summation accurate up to the 9<sup>th</sup> decimal place. On the other hand, we have  $|f_{\pi/t}(t) - f(t)| \leq \|f\|_{\infty} \frac{e^{-2\gamma t}}{1 - e^{-2\gamma t}}$  from (6.2), which is of order  $10^{-10}$ . Finally, the overall error is of order  $10^{-10}$ . Note that, for a fixed  $t$ , the computation cost of  $E(q, N, t)$  is proportional to  $N + q$ .

## 7 Conclusion and further prospects

In this paper, we have proposed a very simple and natural extension of the Black-Cox model. It is an hybrid model, and contrary to hitting time models, it has a non-zero default intensity away from the threshold. Besides, the parameters have a clear heuristic meaning. The strength of this Black-Cox extension is that the cumulative distribution function of the default time remains known explicitly through its Laplace transform. This allows to instantaneously compute CDS prices and their sensitivities to the model parameters. It especially enables to get a quick way to calibrate the parameters to the CDS data. As shown in Section 4, considering the model with only one barrier is sufficient to correctly fit a wide range of CDS spread curves. Nonetheless, one has to be careful because even though this calibration generally leads to a correct fit of the default distribution, it may happen that the parameters themselves are not meaningful. Two significantly different parameter sets can give similar CDS spreads, and one has to get further information to neatly fit the parameters.

In our study, we have considered the parameters of the model as free parameters and we have fitted them to CDS market prices. Doing so, it is calibrated under a risk-neutral probability and can be used for pricing and hedging purposes. However, it is also possible to have a “structural approach” and to determine the model parameters by analyzing firm’s economic data. Thus, it would be interesting to determine from the balance sheet of a firm what the value of  $V_0$  and of the other different model parameters would be. In that case, the thresholds  $C_i$  could be related to credit events of the firm or to some critical firm values around which its policy has to be changed. This would give an interesting way of estimating the default probabilities under the historical probability measure. A possible

way of implementing this would be to consider the rating of the firm by an agency, and associate to each rating a default intensity  $\mu_i$ . Then, the barriers  $C_i$  and the parameter  $\alpha$  would be obtained from the balance sheet of the firm by some economical analysis. This kind of structural approach for the calibration would be of course also really interesting. However, it obviously requires additional data and expertise in economic analysis, and we leave it for future work.

Another interesting continuation of this work would be to study how this model can be used in the multiname setting using the so-called bottom-up approach (see for example Bielecki et al. [3]). More precisely, let us consider a basket of default times and let us assume that the underlying firm values follow a multidimensional Black-Scholes model. We have explained in this paper how it is possible to fit the CDS data of each basket component with one barrier. Once we have fitted  $C$ ,  $\alpha$ ,  $\mu_1$  and  $\mu_2$  for each firm, we would like to fit the whole model to multiname products such as CDO tranches. To do so, one has to calibrate the correlation matrix between the firm values and, if necessary, the dependency between the exponential variables, which trigger the default times. However, the correlation matrix of the firm values is also closely related to the one of the stocks. Ideally, one would like to find a calibration procedure that is both consistent with equity and credit markets. More simply, this kind of model could make a bridge between these markets and qualitatively compare how they price the dependency between companies.

## A Mathematical properties of the cdf of $\tau$

The scope of this section is to state some mathematical properties of the cumulative distribution function of  $\tau$ . We will denote by

$$\Pi_n = \{(\mathbf{b}, m, \boldsymbol{\mu}) \in \mathbb{R}^{n-1} \times \mathbb{R} \times \mathbb{R}_+^n, b_1 > \dots > b_{n-1}, \mu_1 < \dots < \mu_n\},$$

the set of admissible parameters in a setting with  $n - 1$  barriers. We recall the convention  $b_0 = +\infty$  and  $b_n = -\infty$ .

### A.1 Basic properties and regularity w.r.t parameters

First, we state a result on the monotonicity with respect to each parameter.

**Proposition A.1.** *For any  $t \geq 0$ , the function  $P_{\mathbf{b}, m, \boldsymbol{\mu}}(t)$  is nondecreasing with respect to each  $b_i$  and each  $\mu_i$ , and is nonincreasing with respect to  $m$ .*

*Proof.* From (9),  $P_{\mathbf{b}, m, \boldsymbol{\mu}}(t) = 1 - \mathbb{E} \left[ e^{-\int_0^t \sum_{i=1}^n \mu_i \mathbf{1}_{\{b_i \leq W_s + ms < b_{i-1}\}} ds} \right]$ . It is then sufficient to observe that  $\sum_{i=1}^n \mu_i \mathbf{1}_{\{b_i \leq x < b_{i-1}\}} = \mu_1 + \sum_{i=1}^{n-1} (\mu_{i+1} - \mu_i) \mathbf{1}_{\{x < b_i\}}$  is nonincreasing w.r.t  $x$ , nondecreasing w.r.t. each  $\mu_i$  for  $i = 1, \dots, n$ , and nondecreasing w.r.t. each  $b_i$  for  $i = 1, \dots, n - 1$  thanks to (5).  $\square$

In the calculation of the Laplace transform in Theorem 2.1, we have obtained different formulas according to the integer  $i$  such that  $b_i \leq 0 < b_{i-1}$ . However,  $P_{\mathbf{b}, m, \boldsymbol{\mu}}(t)$  and

its derivatives w.r.t each parameter are continuous functions of  $(\mathbf{b}, m, \boldsymbol{\mu})$ . This feature is important when dealing with calibration, since we will use a gradient algorithm to minimize some distance between the real and theoretical prices: there is no discontinuity when crossing barriers (i.e. when  $\exists i \in \{1, \dots, n-1\}, b_i = 0$ ).

**Proposition A.2.** *The function  $P_{\mathbf{b}, m, \boldsymbol{\mu}}(t)$  is continuous w.r.t.  $(\mathbf{b}, m, \boldsymbol{\mu}) \in \Pi_n, t \geq 0$ . It has derivative w.r.t.  $b_i, i = 1, \dots, n-1$  (resp.  $m$  and each  $\mu_i, i = 1, \dots, n$ ) and  $\partial_{b_i} P_{\mathbf{b}, m, \boldsymbol{\mu}}(t)$  (resp.  $\partial_m P_{\mathbf{b}, m, \boldsymbol{\mu}}(t)$  and  $\partial_{\mu_i} P_{\mathbf{b}, m, \boldsymbol{\mu}}(t)$ ) is continuous w.r.t.  $(\mathbf{b}, m, \boldsymbol{\mu}) \in \Pi_n$  and  $t \geq 0$ .*

*Proof.* We set for  $t \geq 0$ ,

$$\left. \frac{d\tilde{\mathbb{P}}}{d\mathbb{P}} \right|_{\mathcal{G}_t} = \exp(-mW_t - m^2t/2),$$

so that  $(\tilde{W}_s = W_s + ms, s \in [0, t])$  is a Brownian motion under  $\tilde{\mathbb{P}}$ . We get from (9) by using Girsanov's Theorem:

$$\begin{aligned} P_{\mathbf{b}, m, \boldsymbol{\mu}}^c(t) &= e^{-\mu_1 t} \mathbb{E} \left[ e^{-\int_0^t \sum_{i=1}^{n-1} (\mu_{i+1} - \mu_i) \mathbf{1}_{\{W_s + ms < b_i\}} ds} \right] \\ &= e^{-\mu_1 t} \tilde{\mathbb{E}} \left[ e^{m\tilde{W}_t - m^2t/2} e^{-\int_0^t \sum_{i=1}^{n-1} (\mu_{i+1} - \mu_i) \mathbf{1}_{\{\tilde{W}_s < b_i\}} ds} \right] \\ &= e^{-\mu_1 t} \tilde{\mathbb{E}} \left[ e^{m\tilde{W}_t - m^2t/2} e^{-\sum_{i=1}^{n-1} (\mu_{i+1} - \mu_i) \int_{-\infty}^{b_i} \tilde{\ell}_t(x) dx} \right], \end{aligned}$$

where  $\tilde{\ell}_s(x)$  denotes the local time associated to  $(\tilde{W}_s, s \in [0, t])$  and is continuous with respect to  $(s, x)$ . Therefore, it is continuous w.r.t.  $(\mathbf{b}, m, \boldsymbol{\mu}) \in \Pi_n$  and  $t \geq 0$ . Moreover, for each parameter, we can differentiate inside the expectation using Lebesgue's theorem and the derivative is continuous w.r.t.  $(\mathbf{b}, m, \boldsymbol{\mu}) \in \Pi_n$  and  $t \geq 0$ , which yields the result.  $\square$

## A.2 Time regularity when $n = 2$

In order to study the accuracy of the different algorithms presented in Section 4 to numerically invert the Laplace transform of  $\tau$ , it is essential to know how regular the distribution function can be expected to be. Our analysis relies on the formula of the Laplace transform (4). This is why we only consider here the case  $n = 2$ .

**Proposition A.3.** *When  $b \neq 0$ , the functions  $P_{b, m, \mu_1, \mu_2}(t)$  and  $\partial_p P_{b, m, \mu_1, \mu_2}(t)$  for  $p \in \{b, m, \mu_1, \mu_2\}$  are of class  $\mathcal{C}^\infty$  on  $[0, \infty)$ . Moreover, for any  $\varepsilon > 0$ , we have*

$$\forall k \in \mathbb{N}^*, P_{b, m, \mu_1, \mu_2}^{(k)}(t) \underset{t \rightarrow \infty}{=} O(e^{(\varepsilon - \mu_1)t}) \text{ and } \forall k \in \mathbb{N}, \partial_p P_{b, m, \mu_1, \mu_2}^{(k)}(t) \underset{t \rightarrow \infty}{=} O(e^{(\varepsilon - \mu_1)t}).$$

*In particular, these functions are bounded on  $\mathbb{R}_+$  when  $\mu_1 > 0$ .*

*When  $b = 0$ ,  $P_{0, m, \mu_1, \mu_2}$  is of class  $\mathcal{C}^1$  on  $[0, \infty)$  but not  $\mathcal{C}^2$  and of class  $\mathcal{C}^\infty$  on  $(0, \infty)$ .*

**Remark A.4.** *Since  $P_{b, m, \mu_1, \mu_2}$  is at least of class  $\mathcal{C}^1$  on  $[0, \infty)$ ,  $\forall t < \infty \quad \mathbb{P}(\tau = t) = 0$ .*

*Proof of Proposition A.3.* First, we consider the case  $b \neq 0$ .

$\boxed{b \neq 0}$ : From Theorem 1.1, we know that the Laplace transform of  $P_{b,m,\mu_1,\mu_2}$  is given by

$$\begin{aligned} L_{b,m,\mu_1,\mu_2}(z) &= e^{mb-|b|\sqrt{2(z+\mu_b)+m^2}} \left( \frac{1}{z+\mu_1} - \frac{1}{z+\mu_2} \right) \times \left\{ -\mathbf{1}_{\{b>0\}} \right. \\ &\quad \left. + \frac{-m + \sqrt{2(z+\mu_2)+m^2}}{\sqrt{2(z+\mu_1)+m^2} + \sqrt{2(z+\mu_2)+m^2}} \right\} + \frac{1}{z} - \frac{1}{z+\mu_b}. \end{aligned}$$

We notice that  $\frac{1}{z} - \frac{1}{z+\mu_b}$  is the Laplace transform of the cumulative density function of the exponential distribution with parameter  $\mu_b$ .

For any  $\varepsilon - \mu_1 > \gamma > -\mu_1$ , we have

$$\begin{aligned} P_{b,m,\mu_1,\mu_2}(t) &= (1 - e^{-\mu_b t}) \mathbf{1}_{\{t \geq 0\}} + \frac{1}{2\pi i} \int_{-\infty}^{\infty} e^{(\gamma+is)t} e^{mb-|b|\sqrt{2(\gamma+is+\mu_b)+m^2}} \\ &\quad \left( \frac{1}{\gamma+is+\mu_1} - \frac{1}{\gamma+is+\mu_2} \right) \times \left\{ -\mathbf{1}_{\{b>0\}} \right. \\ &\quad \left. + \frac{-m + \sqrt{2(\gamma+is+\mu_2)+m^2}}{\sqrt{2(\gamma+is+\mu_1)+m^2} + \sqrt{2(\gamma+is+\mu_2)+m^2}} \right\} ds \end{aligned}$$

The function  $s \mapsto s^k e^{(\gamma+is)t} e^{mb-|b|\sqrt{2(\gamma+is+\mu_b)+m^2}} \left( \frac{1}{\gamma+is+\mu_1} - \frac{1}{\gamma+is+\mu_2} \right) \times \left\{ -\mathbf{1}_{\{b>0\}} + \frac{-m + \sqrt{2(\gamma+is+\mu_2)+m^2}}{\sqrt{2(\gamma+is+\mu_1)+m^2} + \sqrt{2(\gamma+is+\mu_2)+m^2}} \right\}$  is integrable and continuous on  $\mathbb{R}$  for all  $k \in \mathbb{N}$ , since  $\operatorname{Re} \left( \sqrt{2(\gamma+is+\mu_b)+m^2} \right) \underset{|s| \rightarrow +\infty}{\sim} \sqrt{s}$ . Hence, the function  $P_{b,m,\mu_1,\mu_2}$  is of class  $\mathcal{C}^\infty$  which implies that the random variable  $\tau$  admits a density w.r.t Lebesgue's measure and moreover for every  $k \in \mathbb{N}^*$  and all  $t \geq 0$

$$\begin{aligned} P_{b,m,\mu_1,\mu_2}^{(k)}(t) &= -(-\mu_b)^k e^{-\mu_b t} + \frac{1}{2\pi i} \int_{-\infty}^{\infty} e^{ist} (\gamma+is)^k e^{\gamma t} e^{mb-|b|\sqrt{2(\gamma+is+\mu_b)+m^2}} \\ &\quad \left( \frac{1}{\gamma+is+\mu_1} - \frac{1}{\gamma+is+\mu_2} \right) \times \left\{ -\mathbf{1}_{\{b>0\}} \right. \\ &\quad \left. + \frac{-m + \sqrt{2(\gamma+is+\mu_2)+m^2}}{\sqrt{2(\gamma+is+\mu_1)+m^2} + \sqrt{2(\gamma+is+\mu_2)+m^2}} \right\} ds \end{aligned}$$

Using the Riemann-Lebesgue lemma ( $\int_{-\infty}^{+\infty} f(s) e^{ist} ds \xrightarrow{t \rightarrow +\infty} 0$  if  $f$  is integrable), we get that

$P_{b,m,0,\mu}^{(k)}(t) = O(e^{\gamma t})$  when  $t \rightarrow \infty$ . By differentiating this equation with respect to each parameter, we also get that  $\partial_b P_{b,m,0,\mu}^{(k)}(t)$ ,  $\partial_m P_{b,m,\mu_1,\mu_2}^{(k)}(t)$ ,  $\partial_{\mu_1} P_{b,m,0,\mu}^{(k)}(t)$  and  $\partial_{\mu_2} P_{b,m,0,\mu}^{(k)}(t)$  are

$O(e^{\gamma t})$ .

$\boxed{b=0}$ : Whereas when  $b \neq 0$ , the proof is based on the integrability of the Laplace transform given in Theorem 1.1, to treat the case  $b = 0$ , we use the expression of  $P_{0,m,0,\mu}^c$  given by:

$$\begin{aligned} P_{0,m,0,\mu}^c(t) &= e^{-\mu t}(1 - e^{-m^2 t/2}) + \frac{1}{\pi} \int_0^t \frac{e^{-(\mu+m^2/2)s}}{\sqrt{s}} \frac{e^{-m^2(t-s)/2}}{\sqrt{t-s}} ds \\ &+ \frac{m}{\sqrt{2\pi}} \left[ - \int_0^t \frac{e^{-(\mu+m^2/2)s}}{\sqrt{s}} \Phi(m\sqrt{t-s}) e^{-\mu(t-s)} ds + \frac{1}{\mu} \int_0^t \frac{e^{-m^2 s/2} - e^{-(\mu+m^2/2)s}}{\sqrt{s^3}} \Phi(m\sqrt{t-s}) ds \right. \\ &\left. - \frac{1}{\mu} \int_0^t \frac{e^{-m^2 s/2} - e^{-(\mu+m^2/2)s}}{\sqrt{s^3}} e^{-\mu(t-s)} \Phi(-m\sqrt{t-s}) ds + \int_0^t \frac{e^{-(\mu+m^2/2)s}}{\sqrt{s}} \Phi(-m\sqrt{t-s}) e^{-\mu(t-s)} ds \right]. \end{aligned} \quad (33)$$

Equation (33) can be derived from results of Chesney et al. [11], or one can check that its Laplace transform complies with the one given in (4).

The first term in Equation (33) is obviously of class  $\mathcal{C}^\infty$  on  $[0, \infty)$ . Using the change of variable  $s = tu$ , the second term of Equation (33) can be rewritten

$$\frac{e^{-m^2 t/2}}{\pi} \int_0^1 \frac{e^{-\mu tu}}{\sqrt{u(1-u)}} du$$

and is therefore of class  $\mathcal{C}^\infty$  on  $[0, \infty)$ . Let  $I_1, I_2, I_3, I_4$  respectively denote the last four terms of Equation (33) that are between square brackets. Closely looking at the remaining integrals and performing the same change of variables, it clearly appears that we only have to consider two different types of integrals. For  $\beta, \rho \in \mathbb{R}$ , we introduce

$$J_1(\beta, \rho) = \int_0^1 \frac{e^{\beta tu} \sqrt{t}}{\sqrt{u}} \Phi(\rho\sqrt{t}\sqrt{1-u}) du \quad (34)$$

$$J_2(\beta, \rho) = \int_0^1 \frac{e^{-m^2 tu/2}}{\sqrt{t}\sqrt{u^3}} (1 - e^{-\beta tu}) \Phi(\rho\sqrt{t}\sqrt{1-u}) du. \quad (35)$$

An integration by parts in Equation (34) leads to

$$J_1(\beta, \rho) = \frac{\sqrt{t}}{2} \int_0^1 \frac{e^{\beta tu}}{\sqrt{u}} du + \int_0^1 \left( \int_0^u \frac{e^{\beta tv}}{\sqrt{v}} dv \right) \frac{\rho t e^{-\rho^2 t(1-u)/2}}{2\sqrt{2\pi}\sqrt{1-u}} du.$$

We notice that  $I_1 + I_4 = e^{-\mu t}(-J_1(-m^2/2, m) + J_1(-m^2/2, -m))$ . Hence,

$$I_1 + I_4 = \frac{-mt e^{-\mu t}}{\sqrt{2\pi}} \int_0^1 \left( \int_0^u \frac{e^{-m^2 tv/2}}{\sqrt{v}} dv \right) \frac{e^{-m^2 t(1-u)/2}}{\sqrt{1-u}} du.$$

This new formula makes clear that as a function of  $t$ ,  $I_1 + I_4$  is of class  $\mathcal{C}^\infty$  on  $[0, \infty)$ . The term  $J_2$  is handled by a similar integration by parts:

$$J_2(\beta, \rho) = \frac{1}{2} \int_0^1 \frac{e^{-m^2 tu/2} (1 - e^{-\beta tu})}{\sqrt{t} \sqrt{u^3}} du + \int_0^1 \left( \int_0^u \frac{e^{-m^2 tv/2} (1 - e^{-\beta tv})}{\sqrt{v^3}} dv \right) \frac{\rho}{2\sqrt{2\pi} \sqrt{1-u}} e^{-\rho^2 t(1-u)/2} du$$

As a function of  $t$ , the second integral is clearly of class  $\mathcal{C}^\infty$  on  $[0, \infty)$  from Lebesgue's bounded convergence theorem. Noticing that  $I_2 + I_3 = J_2(\mu, m) + J_2(-\mu, -m) e^{-\mu t}$ ,  $\int_0^1 \frac{e^{-m^2 tu/2} (1 - e^{-\beta tu})}{\sqrt{t} \sqrt{u^3}} du = \int_0^t \frac{e^{-m^2 s/2} (1 - e^{-\beta s})}{\sqrt{s^3}} ds$  and

$$\frac{d}{dt} \left( \int_0^t \frac{e^{-m^2 s/2} (1 - e^{-\mu s})}{\sqrt{s^3}} ds + e^{-\mu t} \int_0^t \frac{e^{-m^2 s/2} (1 - e^{\mu s})}{\sqrt{s^3}} ds \right) = -\frac{\mu e^{-\mu t}}{2} \int_0^t \frac{e^{-m^2 s/2} (1 - e^{\mu s})}{\sqrt{s^3}} ds$$

we get that  $I_2 + I_3$  is (as a function of  $t$ ) of class  $\mathcal{C}^\infty$  on  $(0, \infty)$  but only of class  $\mathcal{C}^1$  on  $[0, \infty)$  and not more. Finally,  $P_{0,m,0,\mu}$  is of class  $\mathcal{C}^\infty$  on  $(0, \infty)$ , but only of class  $\mathcal{C}^1$  on the semi-closed interval  $[0, \infty)$ .  $\square$

## References

- [1] J. Abate, L.G. Choudhury, and G. Whitt. An introduction to numerical transform inversion and its application to probability models. *Computing Probability*, pages 257 – 323, 1999.
- [2] M. Atlan and B. Leblanc. Hybrid equity-credit modelling. *Risk Magazine*, August 2005.
- [3] T. Bielecki, S. Crépey, and M. Jeanblanc. Up and down credit risk. *Preprint*, 2009.
- [4] T. Bielecki and M. Rutkowski. *Credit risk: modelling, valuation and hedging*. Springer Finance. Springer-Verlag, Berlin, 2002.
- [5] F. Black and J. C. Cox. Valuing corporate securities: Some effects of bond indenture provisions. *Journal of Finance*, 31:351–367, 1976.
- [6] D. Brigo and A. Alfonsi. Credit default swap calibration and derivatives pricing with the SSRD stochastic intensity model. *Finance Stoch.*, 9(1):29–42, 2005.
- [7] D. Brigo and M. Morini. Structural credit calibration. *Risk Magazine*, April 2006.
- [8] P. Carr and V. Linetsky. A jump to default extended CEV model: an application of Bessel processes. *Finance Stoch.*, 10(3):303–330, 2006.
- [9] P. Carr and D. Madan. Option pricing and the fast Fourier transform. *Journal of Computational Finance*, 2(4):61–73, 1999.

- [10] A. Chen and M. Suchaneki. Default risk, bankruptcy procedures and the market value of life insurance liabilities. *Insurance Math. Econom.*, 40(2):231–255, 2007.
- [11] M. Chesney, M. Jeanblanc-Picqué, and M. Yor. Brownian excursions and Parisian barrier options. *Adv. in Appl. Probab.*, 29(1):165–184, 1997.
- [12] J. W. Cooley and J. W. Tukey. An algorithm for the machine calculation of complex Fourier series. *Math. Comp.*, 19:297–301, 1965.
- [13] G. Dorfleitner, P. Schneider, and T. Veza. Flexing the default barrier. <http://ssrn.com/abstract=1343513>, 2008.
- [14] I. Karatzas and S. Shreve. *Brownian motion and stochastic calculus*, volume 113 of *Graduate Texts in Mathematics*. Springer-Verlag, New York, second edition, 1991.
- [15] C. Labart and J. Lelong. Pricing double barrier Parisian options. *International Journal of Theoretical and Applied Finance*, 12(1), 2009.
- [16] R. C. Merton. On the pricing of corporate debt: The risk structure of interest rates. *Journal of Finance*, 29(2):449–70, May 1974.
- [17] F. Moraux. Valuing corporate liabilities when the default threshold is not an absorbing barrier. <http://ssrn.com/abstract=314404>, 2002. EFMA 2002 London Meetings.
- [18] D. V. Widder. *The Laplace Transform*. Princeton Mathematical Series, v. 6. Princeton University Press, Princeton, N. J., 1941.
- [19] L. Yu. Pricing credit risk as Parisian options with stochastic recovery rate of corporate bonds. Preprint, 2004.
- [20] C. Zhou. The term structure of credit spreads with jump risk. *Journal of Banking & Finance*, 25(11):2015–2040, 2001.